AN EXPERIMENTAL STUDY OF THE FLOW OF A SUBSONIC AND TURBULENT BOUNDARY LAYER OVER A FORWARD-FACING STEP

Thesis by

Robert George Stevenson

Lieutenant, United States Navy

In Partial Fulfillment of the Requirements

For the Degree of

Aeronautical Engineer

California Institute of Technology

Pasadena, California

1969

(Submitted September 23, 1968)

ACKNOWLEDGMENTS

The author is especially grateful to Dr. Edward E. Zukoski for stimulating the interest in this subject, for his guidance and generous help; and to Dr. E. E. Sechler for providing the funds to support this research.

Thanks are also due to the United States Navy for the opportunity to participate in its postgraduate education program; to Mr. Frank T. Linton, for the construction of the test model and excellent preparation of the graphical figures; to the personnel of the Hydrodynamics Laboratory, for their help and suggestions; to Mrs. Roberta Duffy, for typing the manuscript; and to my family for understanding the difficult hours.

ABSTRACT

The incompressible flow over a normal step in a channel was investigated by making measurements of the static wall pressures upstream of the step, on the step face, and downstream of the step. Several parameters were varied in order to determine their influence on the pressure field. These parameters included the free stream velocity, step height, channel height, and the boundary layer thickness. Tests were made using water as the working medium.

The results indicate that the pressure field in the vicinity of the step base is highly dependent on the ratio of step height to boundary layer thickness, and that the far field is influenced strictly by the ratio of channel height to step height. This distinction becomes more clear when the step is at least two times the boundary layer thickness.

TABLE OF CONTENTS

LIST OF SYMBOLS

C_p	$(P-P_o)/(\frac{1}{2}\rho U_o^2)$
$C_{p_{max}}$	maximum value of C_p in the region downstream of the step
$C_{p_{min}}$	minimum value of C_p in the region downstream of the step
C_{p_s}	value of C_p at the first peak in pressure distribution upstream of the step
h	step height
H	channel height
h'	effective step height: $U_1(H-2\delta^*) = U_2(H-\delta^*-h')$
U	speed outside boundary layer
L	length from leading edge of the plate to the step face
P_o	undisturbed pressure far upstream of the step
P	local static pressure on the wall
Re	Reynolds number $(U_o L/\nu)$
ρ	fluid density
ν	kinematic viscosity
δ	boundary layer thickness on plate with no step
δ^*	displacement layer thickness on plate with no step

Subscripts

o	far upstream station
1	step station
2	far downstream station

LIST OF TABLES

LIST OF FIGURES

I. INTRODUCTION

The steady incompressible flow over a forward-facing normal step in a channel may be divided into two regions. These regions are the near field close to the step base and the far field, both upstream and downstream of the step. There are several parameters which may be used to describe and characterize the flow. These include the free stream velocity, step height, channel height, boundary layer thickness, and fluid properties. These dimensional variables may be collected into three non-dimensional parameters which may be used to characterize the pressure field:

1. the ratio of step height to boundary layer thickness (h/δ);

2. the ratio of channel height to step height, referred to as the blockage (H/h) ; and

3. the Reynolds number ($U_o \delta/\nu$) .

One of the purposes for doing this experiment is to determine the effects on the entire pressure field through the variation of the above dimensionless parameters, and, if possible, to characterize the pressure field in each flow region upstream and downstream of the step by one or more of the above dimensionless parameters.

Since the literature did not contain much previous work on this subject, it was felt that further investigations were warranted. Two sources of recent experiments were carefully studied in order to determine which, if any, of the above-mentioned dimensionless parameters might be the most significant.

Bradshaw[1] conducted his tests in a 15 X 10 inch wind tunnel with the step mounted to give a channel height of 10 inches. He did not

give the downstream length of the step. His step heights varied from 1.0 to 2.25 inches with a boundary layer thickness of about 1.3 inches. He concluded that the pressure distribution in front of the step scaled with the boundary layer thickness. There was no consideration of the interference effects on the pressure field; i.e., blockage (H/h) was not considered as a significant parameter.

Taulbee's[2] conclusions were essentially the same. He conducted the tests using an open jet with the step mounted 14 inches aft of the leading edge of a 20-inch flat plate. The top of the step extended 6 inches downstream. His step heights varied from 0.5 inches to 2.0 inches and the boundary layer thickness varied from 0.4 to 0.9 inches. He also concluded that the pressure field could be characterized by the ratio of step height to boundary layer thickness. Although his tests were conducted under different external boundary conditions, interference effects would still be present; however, he did not discuss the influence of the parameter (H/h) and again concluded that boundary layer thickness was the important scale parameter.

After examination of the results of Bradshaw and Taulbee, it seemed apparent that a very significant flow parameter for incompressible flow was being overlooked. It seemed quite logical to assume that the flow field in the vicinity of the step, say 1 or 2 step heights, might be more significantly influenced by the ratio of step height to boundary layer thickness. However, one might also expect that the far upstream pressure field would be fixed by the external geometry. Very simple calculations for the potential flow solution of

flow over a step in a channel show that the presence of the step is felt far upstream and that the solution is dependent on the ratio of the channel height to step height.

For these reasons, it was deemed necessary to further investigate the incompressible flow over a normal step in a channel in order to determine what influences the ratio of step height to boundary layer thickness, the ratio of channel height to step height, and the Reynolds number had on the pressure field both upstream and downstream of the step.

II. APPARATUS

A. General Description

The test models consisted of forward-facing normal steps mounted on a smooth flat plate. The flat plate was constructed of $\frac{1}{2}$-inch thick aluminum plate, 20 inches wide and 105 inches long. The step face was constructed of 1-inch thick aluminum, spanning the flat plate, with step heights varying from 1/4 inch to 4 inches. The top of the step was constructed of 1/2-inch lucite, 20 inches wide and 37 inches long. Centerline static-pressure taps were located on the flat plate, step face, and top of step, as shown in Tables I and II and Figure 1. There were also spanwise pressure taps located 5 inches either side of centerline, 3/4, 12, and 25 inches in front of the step face, and 1 3/4 and 12 1/4 inches aft of the step face. Probing ports for obtaining velocity profiles were located 1 inch off centerline along the length of the flat plate. No probing ports were placed on top of the step. There were no pressure taps on the step face and step top for the 1/4-inch and 1/2-inch step heights.

The test model was inserted in the free-surface water-tunnel facility of the Hydrodynamics Laboratory. The free-surface water tunnel is a closed-circuit tunnel capable of speed 0 to 30 ft/sec with a 20-inch wide by 30-inch high by 96-inch long test section. The entrance to the test section (which is also the upstream edge of the flat plate) is fitted with a skimmer which removes the free-surface boundary layer produced in the tunnel contraction section so that the boundary layer on the plate starts at the leading edge of the plate. The model was placed inverted on the free surface rather than on the floor of the tunnel

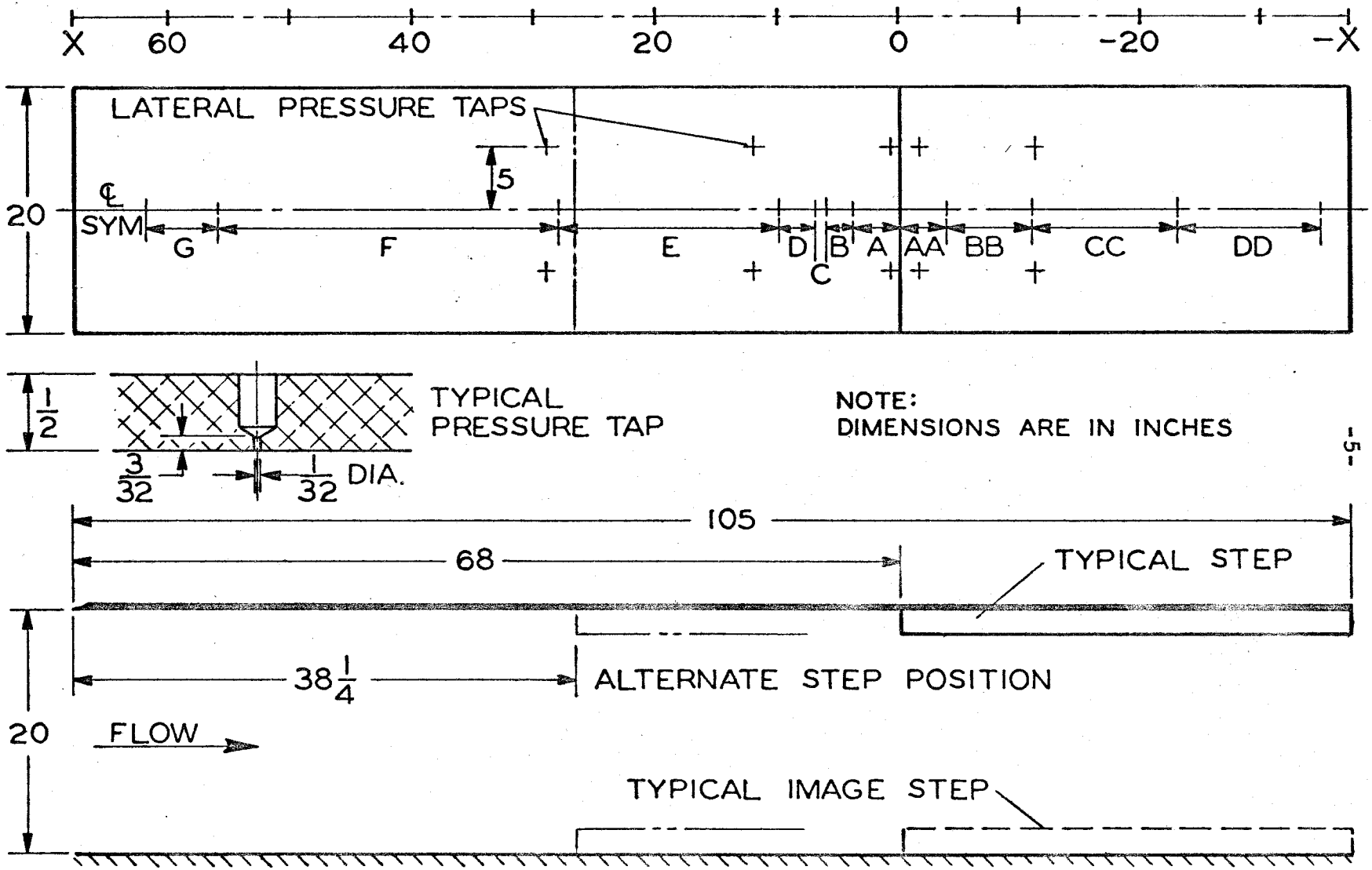

FIG. 1 TEST MODEL SCHEMATIC

DISTANCE OF STEP FROM LEADING EDGE = 68 IN.

	Number of Taps	Spacing (inches)	Schematic* Location
In Front of Step	16	1/4	A $0 \leq x \leq 4$ inch
	4	1/2	B $4 \leq x \leq 6$
	1	1	C $6 \leq x \leq 7$
	2	1 1/2	D $7 \leq x \leq 10$
	9	2	E $10 \leq x \leq 28$
	7	4	F $28 \leq x \leq 56$
	1	6	G $56 \leq x \leq 62$
Top of Step	9	1/2	AA $0 \geq x \geq -4$
	7	1	BB $-4 \geq x \geq -11$
	6	2	CC $-11 \geq x \geq -23$
	3	4	DD $-23 \geq x \geq -35$
1-Inch Step Face	2	1/4	
	1	1/2	
2-Inch Step Face	2	1/4	
	3	1/2	
4-Inch Step Face	2	1/4	
	7	1/2	

* See Figure 1.

TABLE I. PRESSURE TAP DISTRIBUTION

DISTANCE OF STEP FROM LEADING EDGE = 38 1/4 INCHES		
	Number of Taps	Spacing Inches
In Front of Step	8	1/4
	1	1/2
	8	1
	4	2
	2	4
	3	2

TABLE II. PRESSURE TAP DISTRIBUTION

h inches	L inches	H/h	h/δ	U_o (ft/sec)	$Re = U_o L/\nu$
1/4	68	80	.25	5, 10, 15	3×10^6 to 7.8×10^6 for all tests.
1/2	68	40	.50	5, 10, 15	
1	68	20	1.0	5, 10, 15	
1	68	10*	1.0	5, 10, 15	
1	38 1/4	10*	1.33	5, 10, 15	
2	68	10	2.0	5, 10, 15	
2	68	5*	2.0	5, 10	
4	68	5	4.0	5, 10, 15	

*H reduced by use of image step on tunnel floor.

TABLE III. TEST CONFIGURATIONS

in an attempt to eliminate the free surface effects and also for ease in obtaining measurement of pressures. With the test model installed, the cross section of the tunnel upstream of the step was 20 by 20 inches, and, with the step at the rearmost position, the model had a 68-inch flat plate upstream of the step,and a 37-inch flat section formed the step.

The flat plate model was positioned so as to obtain as nearly a zero streamwise pressure gradient as possible with the step removed. With the model fitted, the test section was vented to atmosphere at the downstream end of the flat plate. Figure 1 shows a schematic of the model in the water-tunnel test section and the location and detail of the pressure taps.

B. Measurements

All static wall pressures were measured by water manometers located adjacent to the test section and referenced to atmosphere. A tunnel static reference pressure was obtained from a static pressure tap on the tunnel wall in the undisturbed flow at the entry to the test section. Flat-plate total pressure profiles were measured with a flat Pitot tube, the output of which was fed through a Wianko water-to-air differential pressure transducer to a Non-Linear Systems digital voltmeter. The static wall pressure at each probing station was also fed to the voltmeter.

With the test model in the test section, the tunnel operated in such a manner that the pressure level changed slightly in a periodic manner. However, the period was long enough (seconds) that the manometers had sufficient time to follow accurately the level changes.

This condition existed for all configurations, including the flat plate model, and had no observable influence on measured pressure coefficients.

The majority of the data was obtained with the step positioned 68 inches from the leading edge of the flat plate. This distance was initially selected to avoid any upstream disturbances to the approaching boundary layer and also to ensure that the boundary layer was well-developed and of sufficient thickness. Similarly, the top of the step extended to the downstream baffles at the test section exit in an attempt to reduce the upstream effects of the rearward facing step formed by the termination of the model. Data were also obtained with the step moved forward to a position 38 inches aft of the leading edge.

In order to demonstrate the effects of tunnel wall interference effects, in some of of the tests an "image" step was attached to the bottom wall of the test section at a point exactly opposite the step on the model. This effectively decreased the tunnel test-section depth by a factor of one-half and increased interference effects by a factor of two (i.e., H/h decreased by a factor of 2). By use of the image step it was possible to hold the step height (h) constant and to vary the blockage (H/h), or to hold the blockage constant and vary the step height and step height -to- boundary layer thickness ratio (h/δ). Table III contains the matrix of test configurations in which L represents the flat plate length from the leading edge to the step face and U_o is the free stream velocity.

The flat plate velocity profiles are shown in Figures 2a, 2b, and 2c. From these profiles, the boundary layer thickness was de-

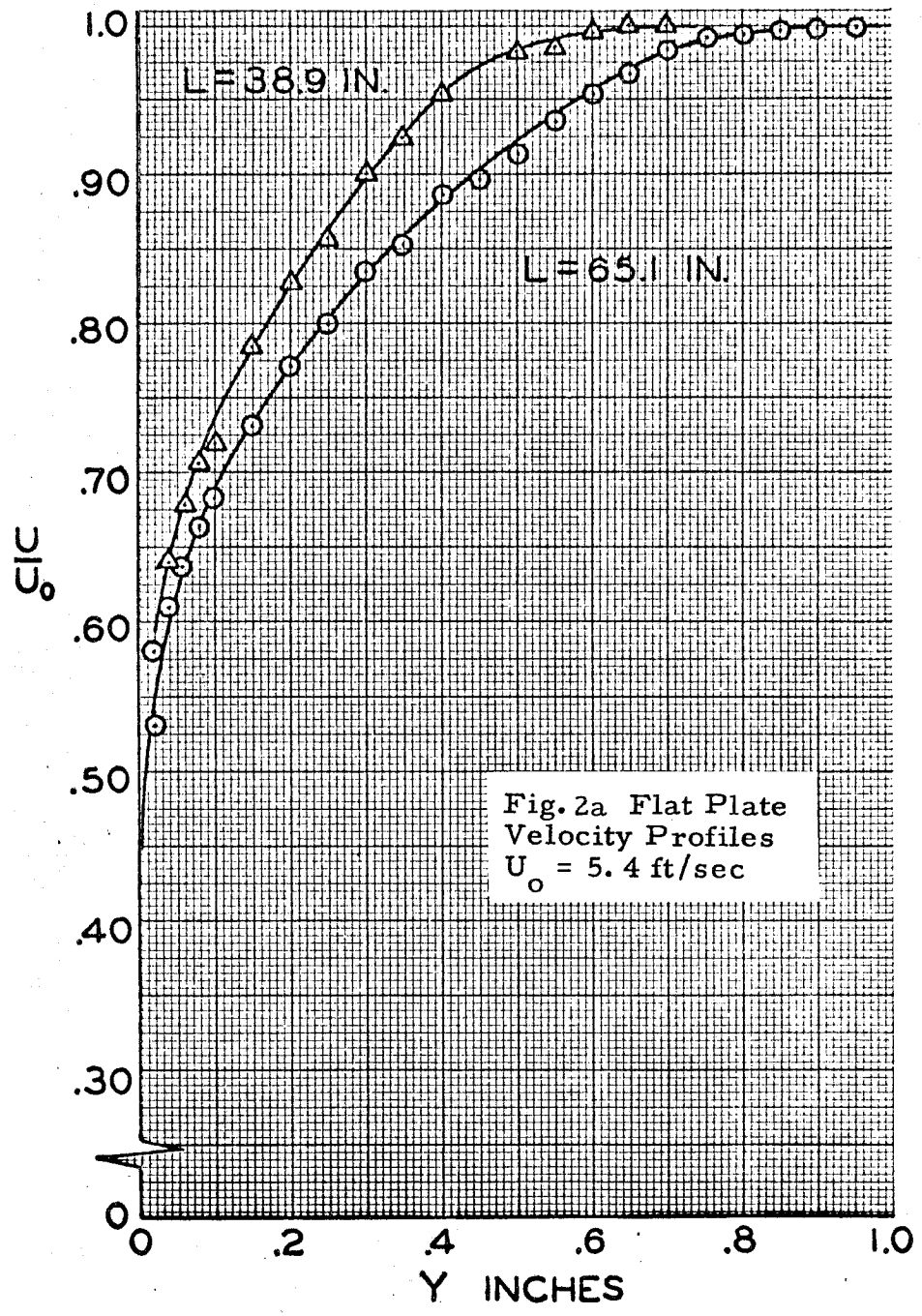

Fig. 2a Flat Plate Velocity Profiles U_o = 5.4 ft/sec

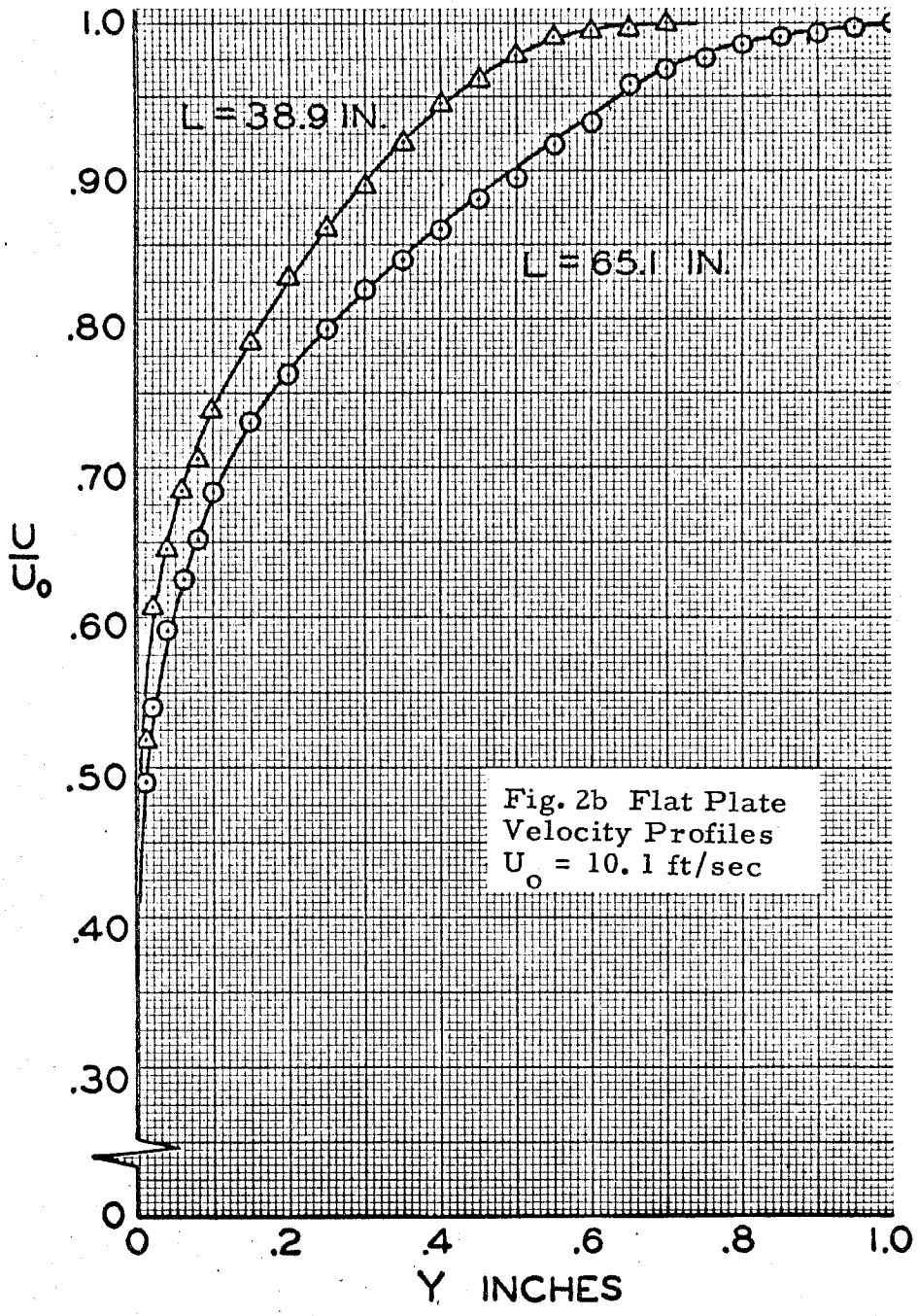

Fig. 2b Flat Plate Velocity Profiles U_o = 10.1 ft/sec

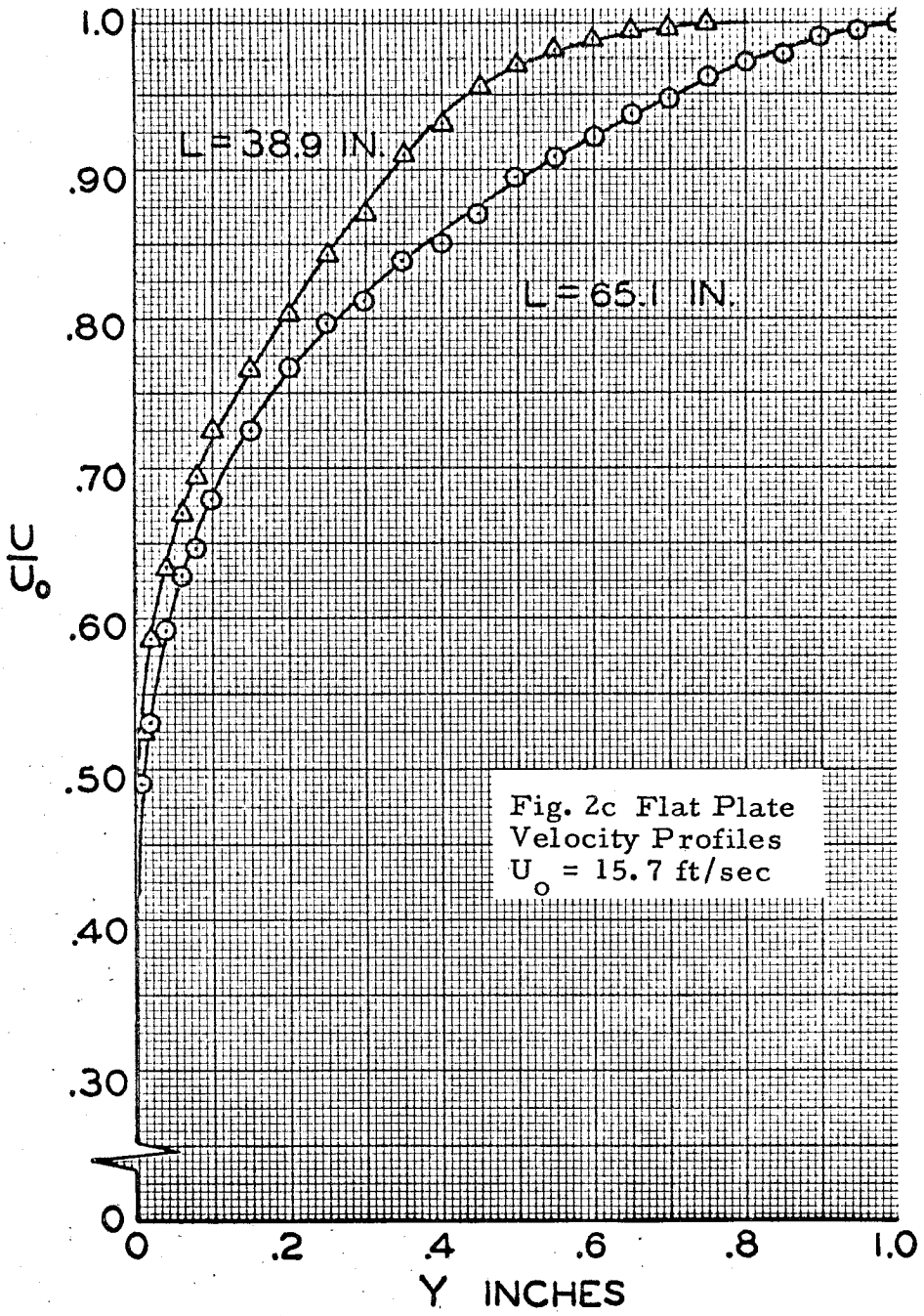

Fig. 2c Flat Plate Velocity Profiles U_o = 15.7 ft/sec

termined to be 3/4 inch at the forward step location (L = 38 inches) and 1 inch at the aft location of the step (L = 68 inches). The Reynolds number, based on the flat plate length (L), varied between 3×10^6 to 7.8×10^6. Because of the nature of the velocity profiles, the range of the Reynolds numbers, and visual observations, the boundary layer was judged to be a fully-developed turbulent layer.

The boundary layer on the tunnel test-section side walls was also of the order of 1 inch. Provisions were made for installing a vertical fence extending upstream and downstream from the step face inboard of each side wall in order to reduce the degree of spanwise flow. However, these were not used after visual inspection of the flow indicated very little spanwise flow. Results presented in Section IV also indicate relatively good two-dimensionality, especially for the 2- and 4-inch step height configurations.

Little emphasis was placed on an accurate determination of the separation points in front of the step or on the reattachment point aft of the step. However, some flow visualization was attempted using air and dye, and photographs were taken of air injection cases. The results of analyzing these photographs and of visual observations are presented and discussed in Section IV.

III. THEORETICAL MODEL

A. Considerations

Attempts were made to construct a mathematical flow field which would represent the actual flow as closely as possible. Three different mathematical models were considered as possible representations for the real flow field whose principal features are shown schematically in Figure 3. The approach stream separates at point A and reattaches at B. Based on visual observations of tracer motions, both separation and reattachment positions are very unsteady. The flow separates again at C and reattaches at D. This reattachment is also very unsteady, and large vortices are periodically shed from this region. Note that some of the notation used in the following discussion is shown in this figure.

The first model was the flow over a forward-facing normal step in a channel. To modify this, a cavitating flat plate in a channel was considered. To further modify the model, a front stagnation region was added to the cavitating flat plate. Figure 4 illustrates the three models considered (A, B, and C, respectively) and compares the pressure fields produced upstream of the step and on the flat plate for a blockage of $H/h = 5$; the experimental results from the 4-inch step height configuration are also shown here. The third model, Model C, discussed extensively below, was more nearly representative of of the far field region, especially for the step heights of 2 and 4 inches (see Section IV). The figure shows the importance of the downstream flow geometry in determining a good mathematical model for the actual flow. This is also illustrated more clearly in Section IV.

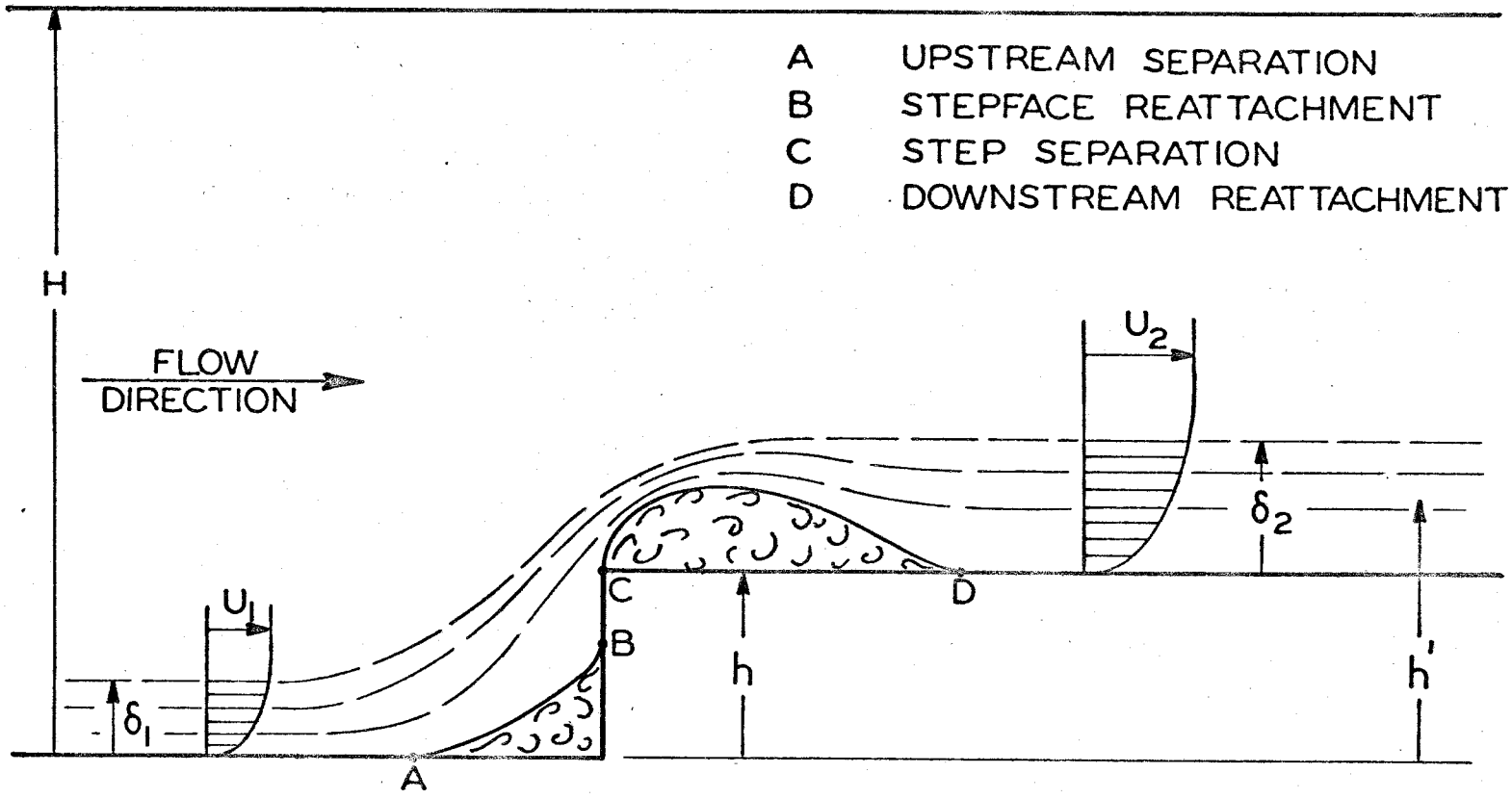

FIG. 3 FLUID FIELD FLOW SCHEMATIC

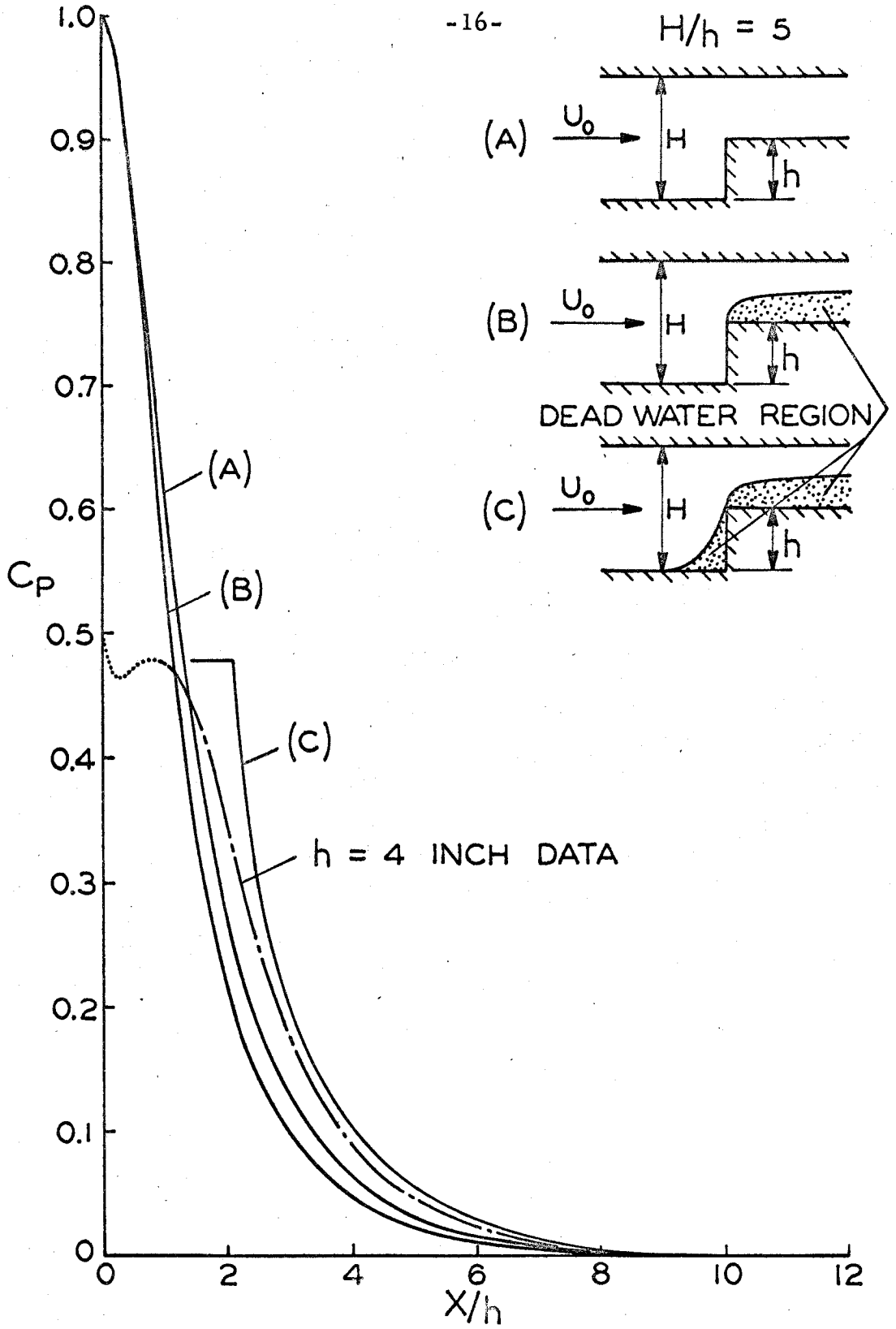

FIG. 4 PRESSURE COEFFICIENT FOR FLOW OVER NORMAL STEP WITH DIFFERENT DOWNSTREAM CONDITIONS

B. Mathematical Model

The two-dimensional model chosen for mathematical analysis is the channel flow shown in Figure 4, and in more detail in Figure 5. Initially, uniform flow with a velocity u_o passes over a flat plate held normal to the channel walls in the center of the channel. Upstream of the plate at point A the centerline streamline has a cusped bifurcation point which is followed by a constant pressure and constant velocity segment between A and B. The region I is a constant pressure "cavity", and the bounding streamline ($\overline{AD}$) is parallel to the plate at both B and C. The pressure in the downstream cavity, region II, is constant, and the constant pressure streamline bounding this region, $\overline{CD}$, becomes parallel to the undisturbed flow direction far downstream of the plate at D. Finally, the velocity is again uniform at D.

In this model, points A and C correspond to separation points and B to a reattachment point. The regions I and II correspond to the separated regions up- and downstream of the step. The half heights for the flat plate, the tunnel, and the dividing streamline at D are h, H, and h', and these correspond to the real step height, tunnel height, and effective step height, respectively.

The velocity and pressure fields for the flow described here are fixed when u_o, P_o, h/H, and one other suitable parameter are fixed. For the present situation, the pressure in region I was chosen as this additional parameter.

The solution to the problem posed above was obtained by making the standard hodograph transformation and by looking for a solution for the complex potential in the hodograph plane which satisfied

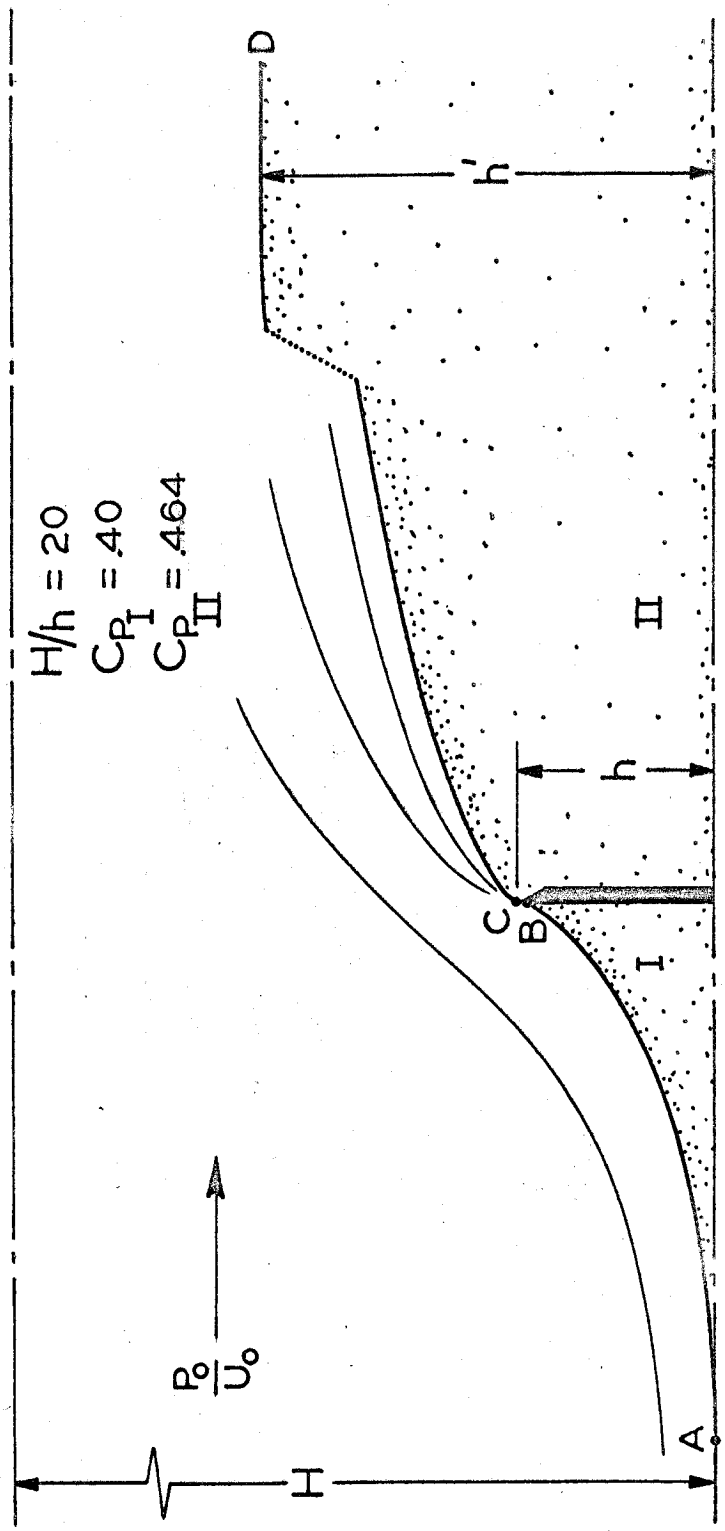

FIG. 5 SCHEMATIC DIAGRAM FOR MATHEMATICAL MODEL

the conditions specified above. A solution was found by the usual technique of superposition of sources and sinks, and was transformed to the real plane by an integral technique. This integration gives the velocity field in the real plane in terms of non-tabulated elliptic functions which could be expressed as rapidly converging infinite series of theta functions.

Numerical values of pressures, pressure coefficients, and the location of the streamline $\overline{ABCD}$ were obtained from a computer program. Although the author was involved in the development of this analysis and carried out the calculations, the model was constructed by Dr. Toshi Kubota and Mr. Robert Gran of the California Institute of Technology, and the computer programming was done by Mr. Gran.

Numerical examples of pressure fields predicted from this model are given later in discussions of the data. However, one general result of the calculations is that the point B lies, within numerical accuracy, at the top of the flat plate or step. That is, the points B and C coincide, and the radii of curvature of the curves $\overline{AB}$ and $\overline{CD}$ at B and C are much less than h.

One of the two inputs to the program was the pressure coefficient in the stagnation region forward of the step, and this was taken from experimental data. Since any discrepancy in this input might significantly influence the results of the model, the curves shown on Figure 6 are presented to illustrate the weak dependence of the pressure field upstream on the pressure or pressure coefficient in the upstream separated region, region I. The extremes of the pressure coefficient obtained from the actual tests are shown, in addition to the

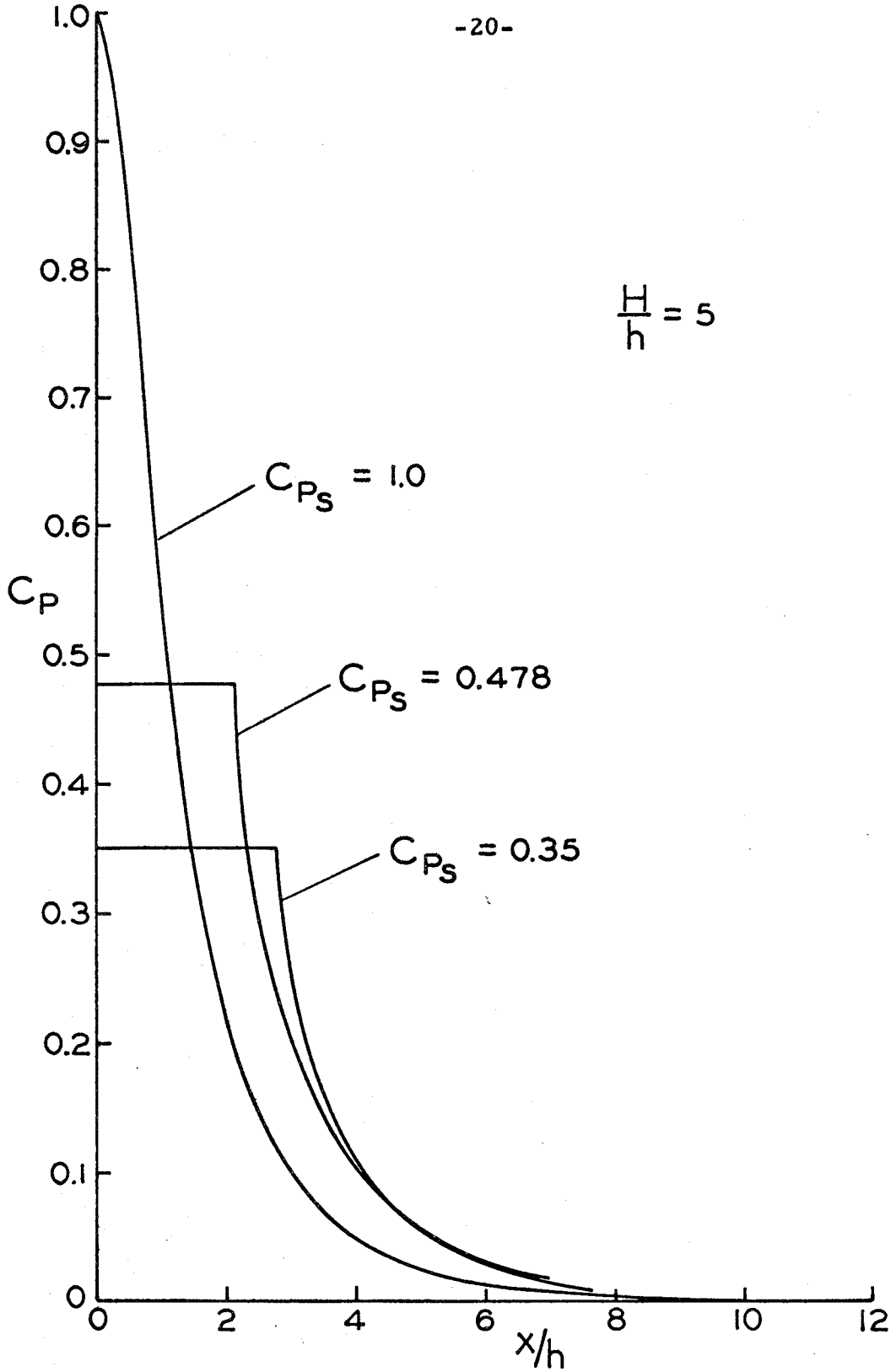

FIG. 6 PRESSURE COEFFICIENT FOR FLOW OVER CAVITATING STEP WITH DEAD WATER REGION IN FRONT

effects when the pressure coefficient becomes unity; i.e., the stagnation region in front of the step vanishes. The point at which the maximum pressure coefficient is first reached may be considered as the separation point for the model. This location is also weakly dependent on the pressure coefficient in region I.

As indicated by comparison of Figures 3 and 5, the mathematical model selected does not represent the real flow field. The downstream conditions appear to be the primary source of error. The real flow field has a cavity which is initially similar to the model, but in the experimental case there exists a definite reattachment of the flow downstream of the step, which is followed by a complex and highly turbulent mixing region extending far downstream.

Lighthill[4] has suggested a fourth model which is applicable to flows for which H/h is infinite. In this model, the points B and C of Figure 3 coincide; the streamline is not parallel to the plate at B or C, and the speed along $\overline{CD}$ is taken to be the undisturbed flow speed. Because in the real flow the reattachment point B lies about h/2 above the centerline, and because interference effects ($H/h < \infty$) are important, the present model appears to be more realistic. In addition, Lighthill's model predicts that the pressure disturbance propagates much farther upstream than was observed experimentally.

IV. RESULTS

A. Data Reduction

Photographic coverage of the large (83-tube) manometer bank was used to obtain the basic pressure data. This coverage was necessary because of a slow variation in tunnel total pressure, $\Delta P \approx 1/4$ inch water with a 2-to 4-second period, which had no effect on the reduced pressures but which made visual monitoring of the tubes unfeasible. This photographic coverage actually facilitated the data reduction because these photographs were interpreted by means of a film reader which was fitted with a potentiometer, which fed a signal to a voltmeter which was linearly proportional to the height of the fluid in each manometer tube. The output of the voltmeter was fed to an IBM punch machine which recorded the data. A very simple computer program was written to calculate the wall pressure coefficients $C_p = [(P-P_o)/(\frac{1}{2}\rho_o U_o^2)]$, and these results were also plotted with the use of the computer. Because of the scale used by the computerized plotter, the data are presented in terms of $x/10$ and $x/10h$ rather than as x or x/h.

Although great care was taken to position the model, without the step, in the water tunnel to obtain a nearly zero streamline pressure gradient, data for the no-step configuration indicated that there did exist a slight pressure gradient for each of the three tunnel speeds. The flat-plate pressure gradient was essentially zero up to about 36 inches forward of the step, at which point there was a uniform rise to a level of $C_p = 0.022$ at about 28 inches forward of the step. The pressure thereafter maintained this level with scatter of less than

$\pm 0.004 q_o$. It was not obvious why this jump occurred on the flat plate, but it appeared at all tunnel speeds, was not caused by flat plate curvature, and could not be removed by changes in plate alignment. Because of restrictions on testing time, tests were continued without further attempts to correct this situation. It should be pointed out, however, that with the exception of the 4-inch step configurations, the upstream influence had diminished to less than a few percent of q prior to the small jump in the flat-plate pressure level.

Because of the inherent operating characteristics of the free-surface water tunnel, it was not possible to control the water level at any constant position for each set of runs. Consequently, for each configuration -- that is, for each step height at the three tunnel speeds -- the static reference pressure shifted according to the water level maintained in the test section. Therefore, in order to place each set of data in a common reference plane, the far-upstream pressure coefficient level was designated as the zero level, and this level was used as the zero pressure in computing values of pressure coefficient. This selection of a final reference pressure was felt to be valid as the upstream influence of the step configurations did not extend to the forward 32 inches of the plate. In summary, each final set of calculations contains a correction due to the variation of the flat-plate (i.e., no-step) pressure coefficient level, which was always less than $0.022 q$, and a correction due to the general pressure level in the tunnel far upstream of the step. With these corrections applied, all figures represent only the effects on the pressure field due to the step disturbance.

B. Data Presentation

The incompressible, steady, and essentially two-dimensional flow over a forward-facing normal step may be characterized by several parameters including the free stream velocity (U_o), step height (h), external geometry (H), boundary layer thickness (δ), and fluid properties (ν). Dimensionless parameters derived from these variables are Reynolds number U_oL/ν, H/h, and h/δ; these were the three parameters varied in the present test. Their ranges are shown in Table III, page 7.

The data are presented and discussed separately for three regions of the flow field: (1) upstream of the step; (2) step face; and (3) on the step top. Although data exist for each of the three speeds tested, only the 15 ft/sec results are presented. The reason for this will be discussed below. However, for some configurations for which sufficient data were not available at 15 ft/sec, the 10 ft/sec results have been presented.

1. Forward of the Step. Figures 7 through 16 present the variations of pressure coefficient with upstream location where x represents the distance measured from the base of the step face. (Again note that x/10 rather than x is used in these figures.) The data are shown for increasing step heights, and h/δ increases from 1/4 to 4 also. All flow conditions are similar with the exception of Figure 10, which has a gas cavity on top of the step beginning at the leading edge of the step face top and extending far downstream. For the other configurations, the flow on top of the step is a recirculatory - mixing regime extending far downstream.

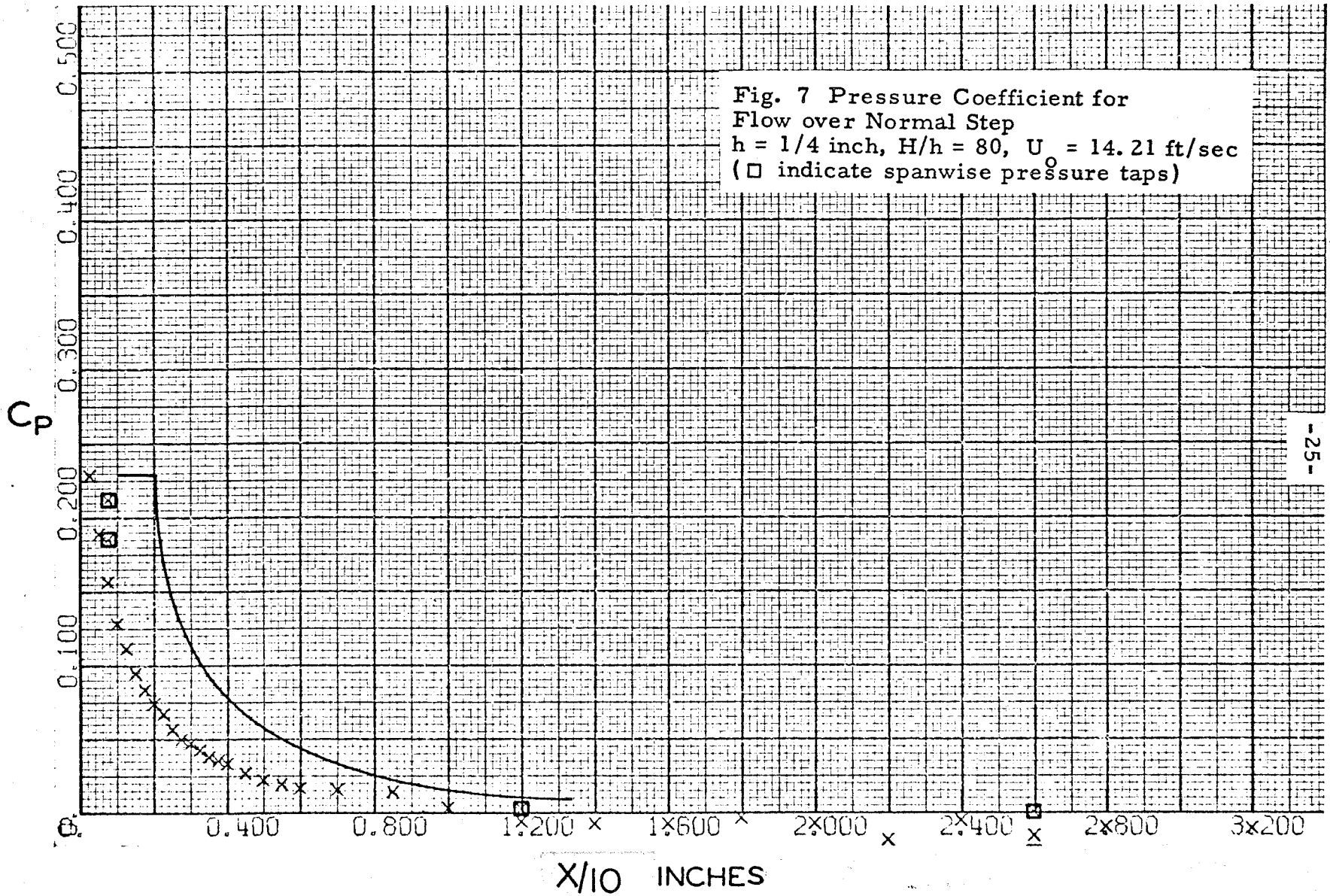

Fig. 7 Pressure Coefficient for Flow over Normal Step
h = 1/4 inch, H/h = 80, U_o = 14.21 ft/sec
(□ indicate spanwise pressure taps)

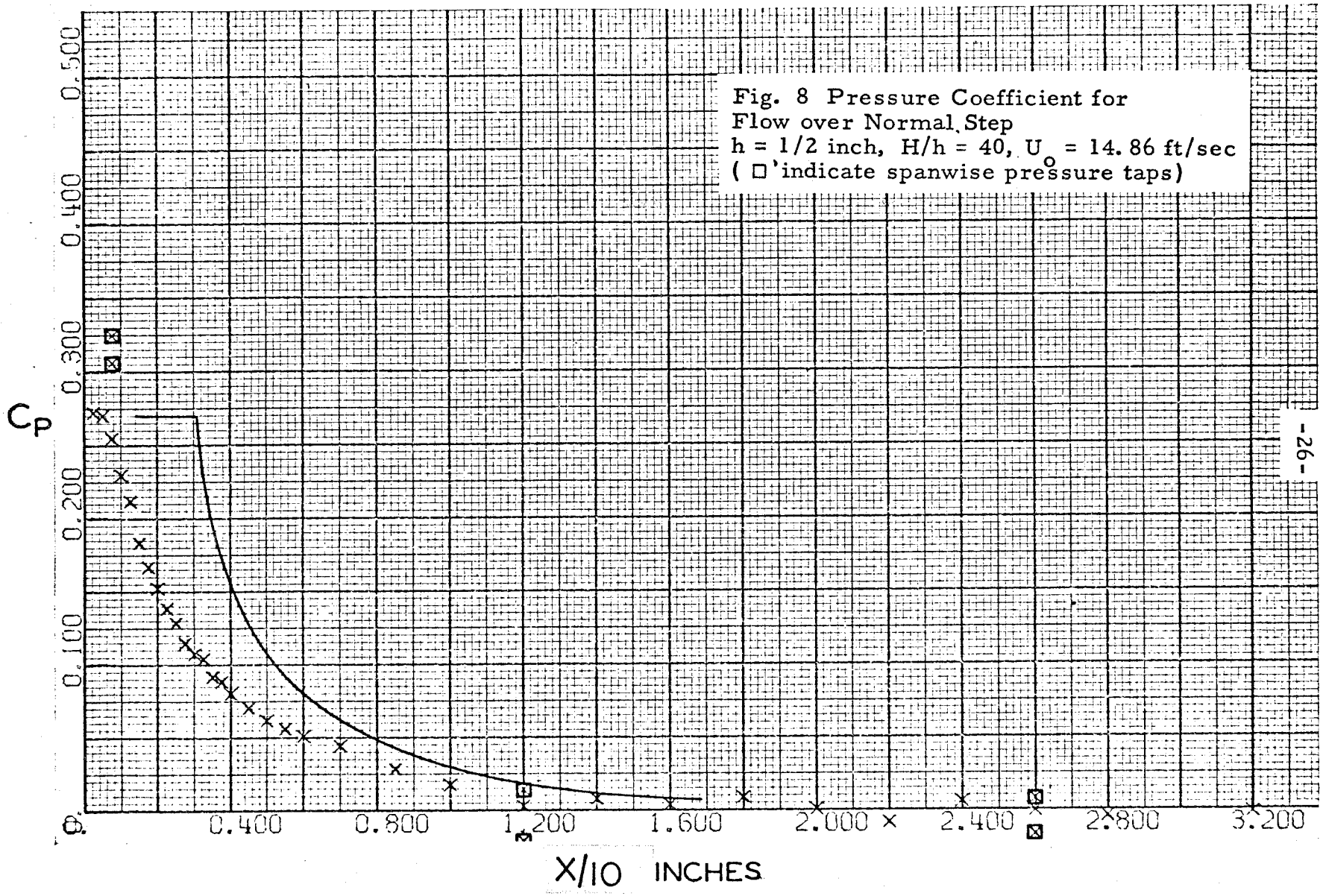

Fig. 8 Pressure Coefficient for Flow over Normal Step
h = 1/2 inch, H/h = 40, U_o = 14.86 ft/sec
(□ 'indicate spanwise pressure taps)

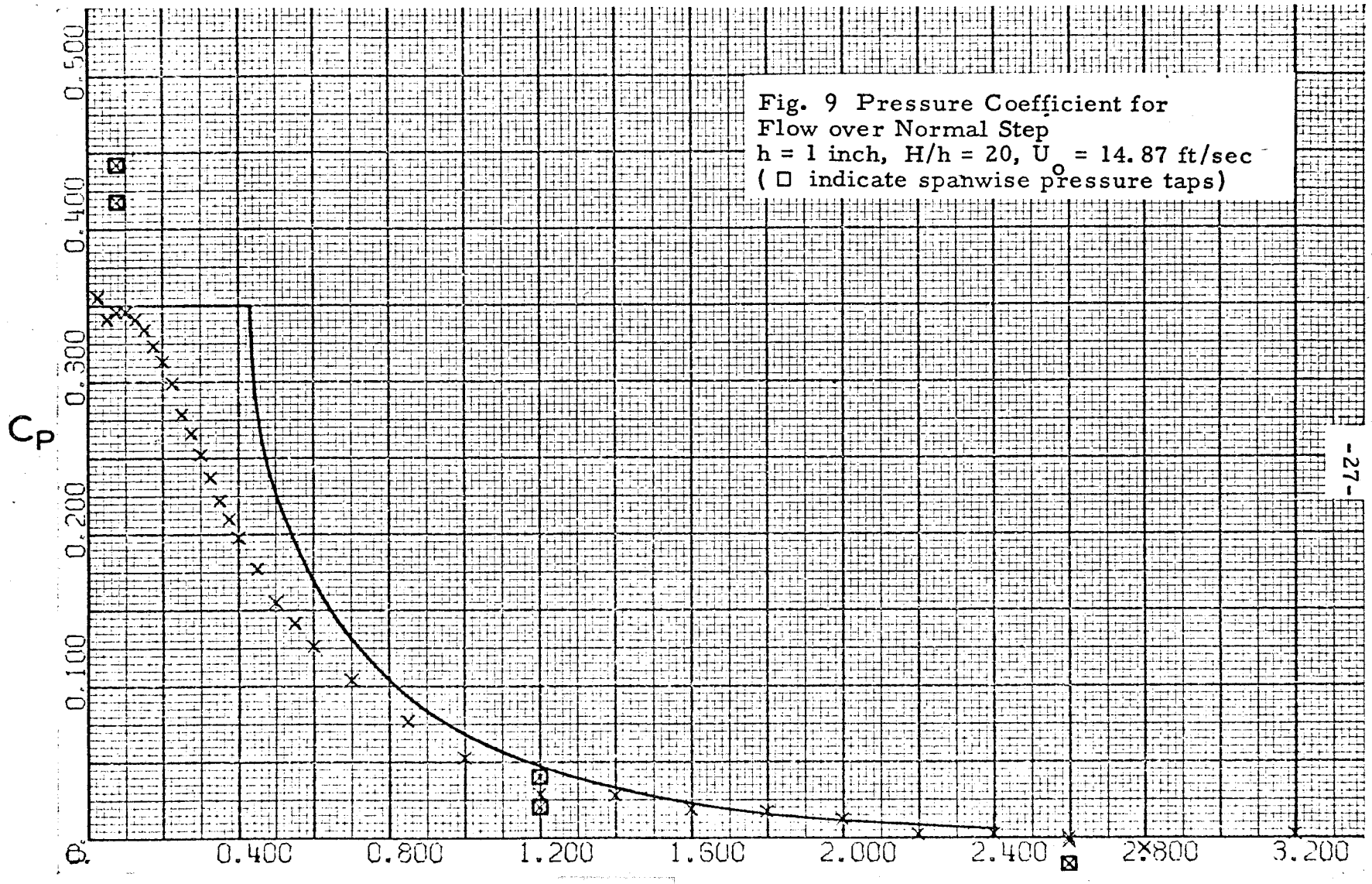
Fig. 9 Pressure Coefficient for
Flow over Normal Step
h = 1 inch, H/h = 20, U = 14.87 ft/sec
(□ indicate spanwise pressure taps)
Cp
0.500
0.400
0.300
0.200
0.100
0.
0.400
0.800
1.200
1.600
2.000
2.400
2.800
3.200
X/10 INCHES

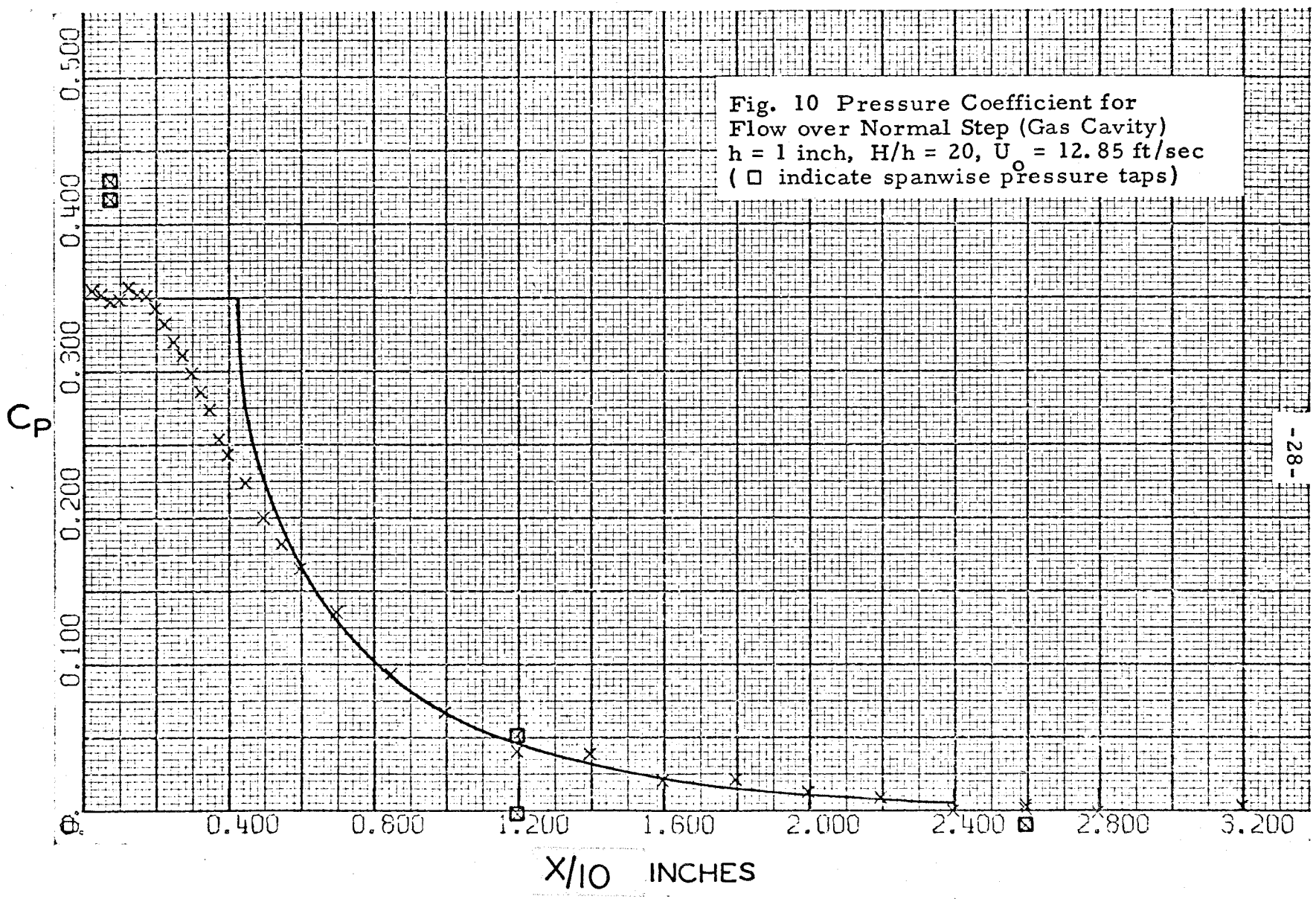

Fig. 10 Pressure Coefficient for Flow over Normal Step (Gas Cavity) h = 1 inch, H/h = 20, U_o = 12.85 ft/sec (☐ indicate spanwise pressure taps)

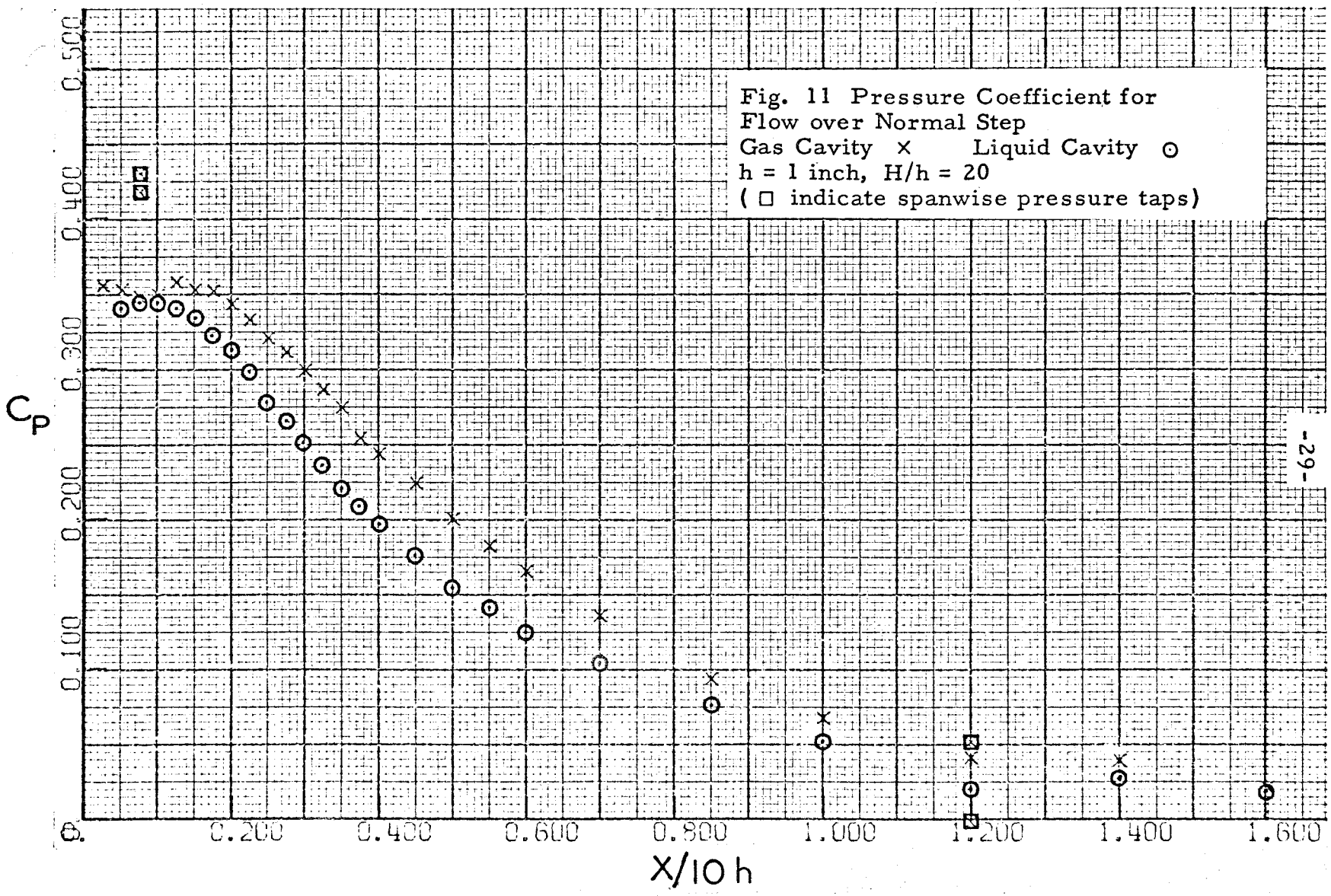
Fig. 11 Pressure Coefficient for
Flow over Normal Step
Gas Cavity × Liquid Cavity ⊙
h = 1 inch, H/h = 20
(□ indicate spanwise pressure taps)
C_p
0.500
0.400
0.300
0.200
0.100
0.
0.200
0.400
0.600
0.800
1.000
1.200
1.400
1.600
X/10 h

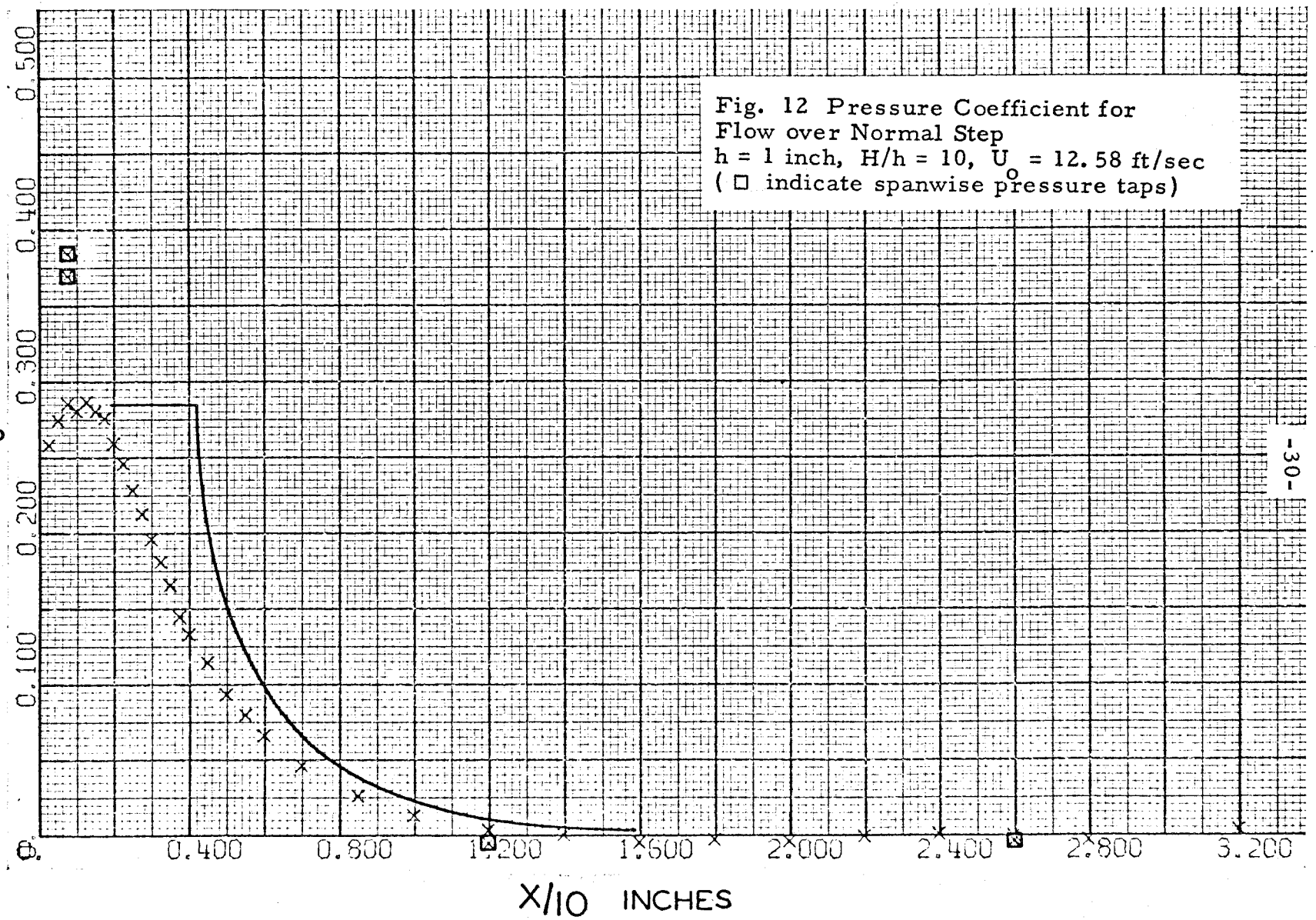

Fig. 12 Pressure Coefficient for Flow over Normal Step
h = 1 inch, H/h = 10, U_o = 12.58 ft/sec
(□ indicate spanwise pressure taps)

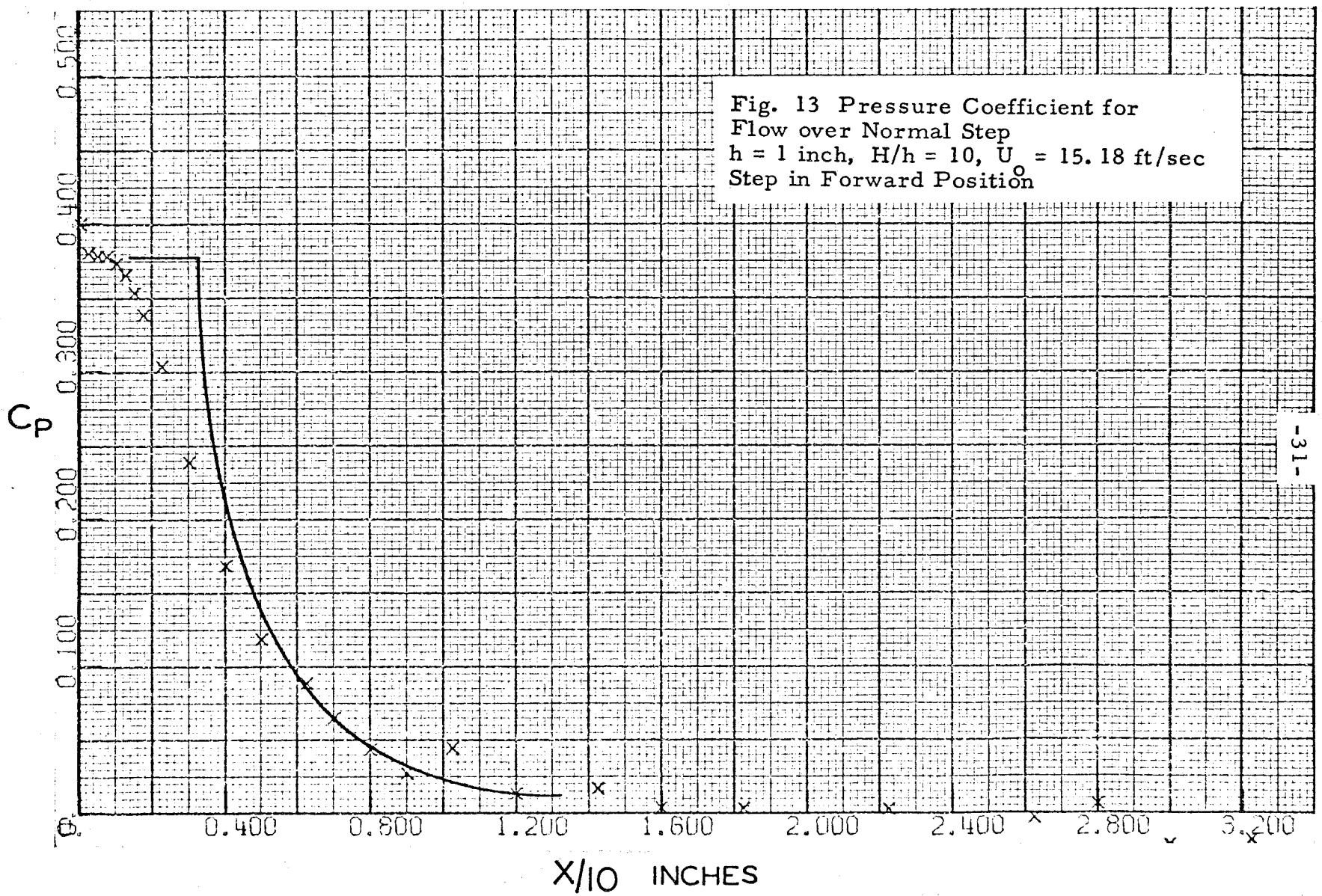

Fig. 13 Pressure Coefficient for
Flow over Normal Step
h = 1 inch, H/h = 10, U_o = 15.18 ft/sec
Step in Forward Position

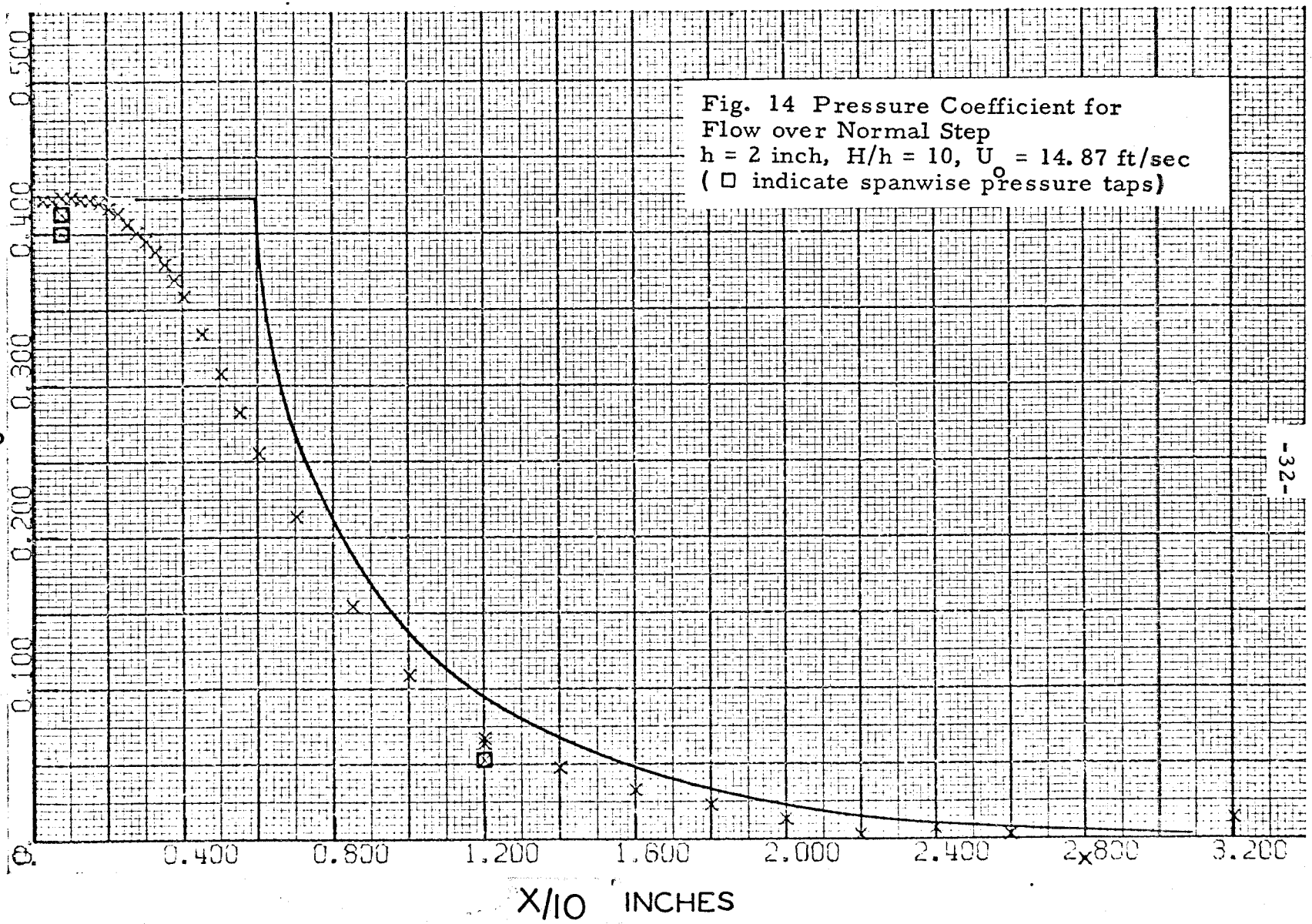

Fig. 14 Pressure Coefficient for Flow over Normal Step
h = 2 inch, H/h = 10, U_o = 14.87 ft/sec
(□ indicate spanwise pressure taps)

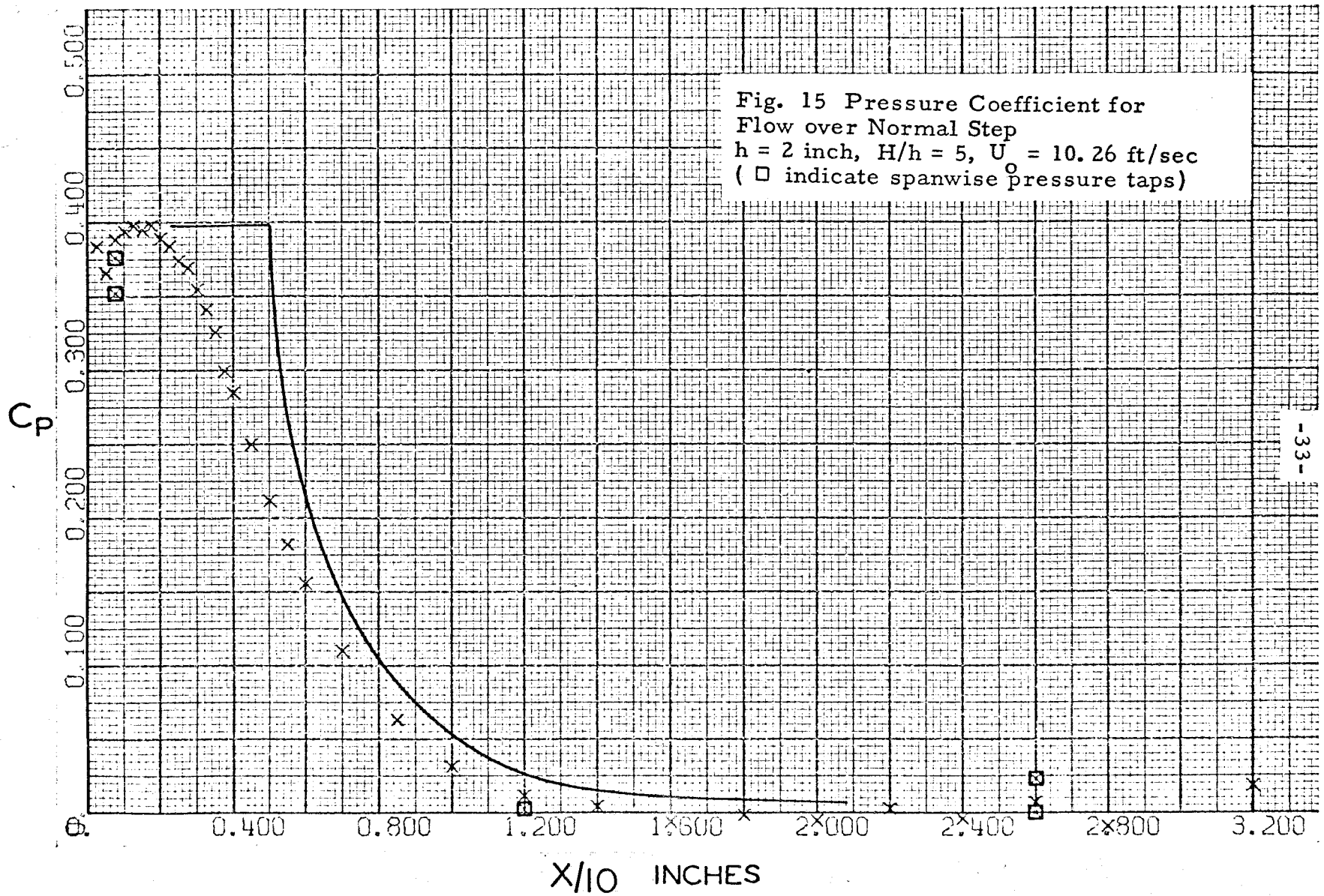
Fig. 15 Pressure Coefficient for
Flow over Normal Step
h = 2 inch, H/h = 5, U_o = 10.26 ft/sec
(□ indicate spanwise pressure taps)
C_P
0.500
0.400
0.300
0.200
0.100
0.
0.400
0.800
1.200
1.600
2.000
2.400
2.800
3.200
X/10 INCHES

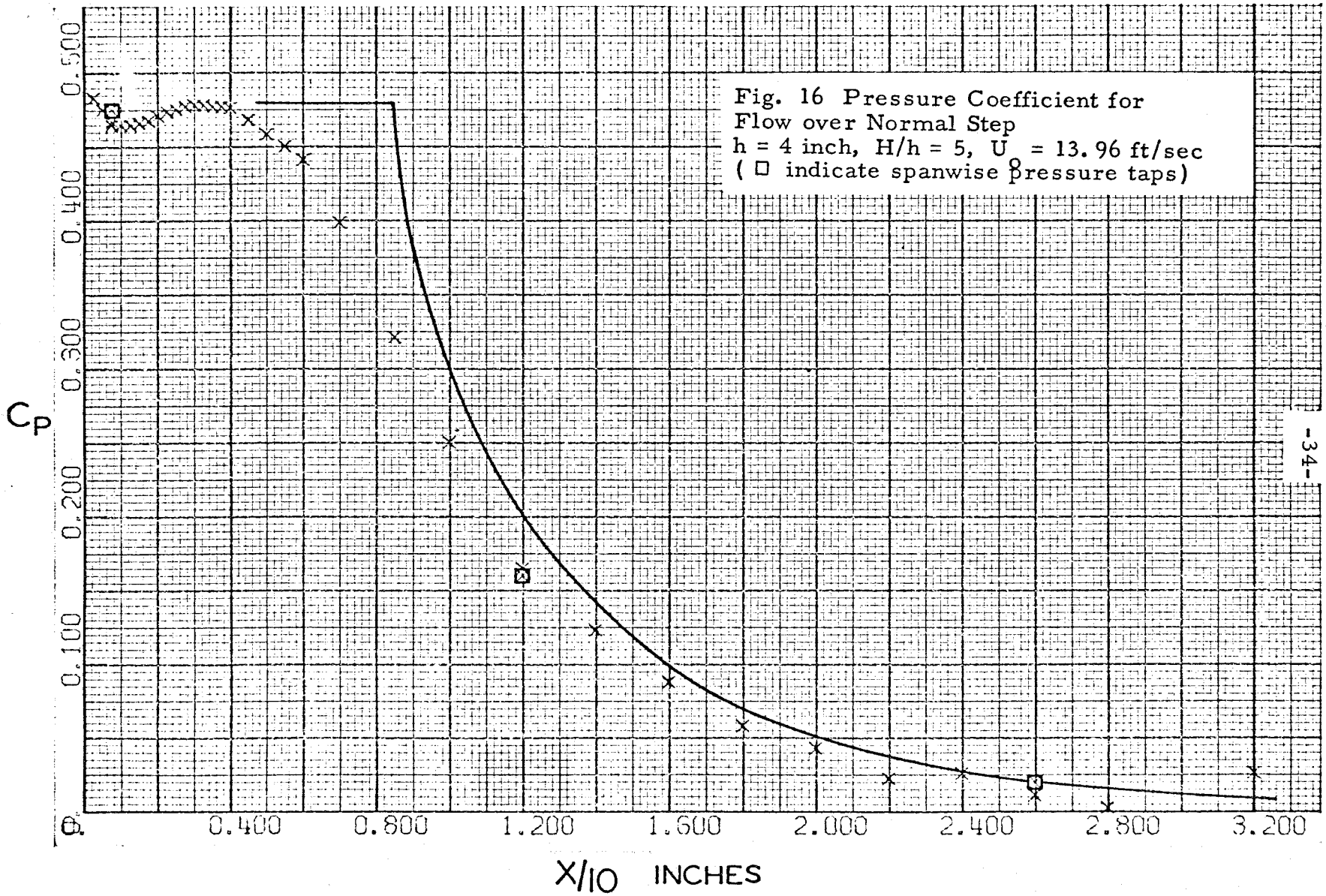
Fig. 16 Pressure Coefficient for
Flow over Normal Step
h = 4 inch, H/h = 5, U∞ = 13.96 ft/sec
(□ indicate spanwise pressure taps)
Cp
0.500
0.400
0.300
0.200
0.100
0
0.400
0.800
1.200
1.600
2.000
2.400
2.800
3.200
X/10 INCHES

Evidence of the degree of two-dimensionality can be seen by observing the data points blocked by the squares, which indicate data obtained from spanwise pressure taps located 5 inches off the centerline or half way to the side walls. Note that the two-dimensionality becomes much better for step heights greater than the boundary layer thickness,and that for h = 4 inches the spanwise pressure gradient is essentially zero. In addition, flow visualization by injection of permanganate solution dye and gas bubbles showed that lateral flows in the recirculation region and farther upstream were too weak to observe for all test configurations. Thus, although lateral pressure gradients were present and weak lateral flows were possible, neither appeared to dominate the flow field.

The solid line in Figures 7 to 16 represents the pressure distribution based on the mathematical model as discussed in Section III. The data for the mathematical model were obtained with input parameters of H/h and experimental values of separation pressure coefficient which were taken to be the initial maximum pressure coefficient for each configuration. The similarity of the mathematical model to the actual data becomes increasingly better as the step height is increased, that is, as the step height becomes much larger than the boundary layer thickness. This is quite evident by comparing Figures 7 and 16. This should be expected, since, for the larger step heights, the boundary layer is less significant, proportionally, and the upstream flow is more greatly influenced by the presence of the step. Thus, the effects of the step propagate farther upstream and become more like a potential flow field; whereas for step heights less than or of the order of the

boundary layer thickness, the flow cannot detect the presence of the step until much nearer the base. Consequently, agreement with the mathematical model is poor.

Note also the difference in the upstream pressure distribution for the 1-inch step with the different downstream configurations (Figure 11). The far upstream influence is the same, and the initial pressure rise is similar; however, the pressure for gas cavity configuration commences a steeper gradient farther in front of the step than does the pressure for the liquid cavity configuration and apparently is not as strongly influenced by the step. Again, this should not be surprising, as the effective step height (based on height of the cavity) for the gas cavity flow is greater than for the liquid cavity flow. For example, $h' = 1.30$ inches for the liquid cavity and $h' = 1.78$ inches for the gas cavity for $H/h = 20$. Both configurations attain about the same maximum pressure. The agreement of the mathematical model is excellent for the case of the downstream gas cavity, which further demonstrates the importance of the downstream flow geometry in obtaining an appropriate mathematical representation for the upstream flow. This point was also noted in Section III. Figure 11 shows that the two cases agree up to about 6 inches in front of the step. This will be discussed further when considering the effects of the various parameters on the overall flow pattern.

As was pointed out previously, the 15 ft/sec data have been presented as representative of the three tunnel speeds for which tests were made. As justification for this, Figure 17 shows the influence of velocity or Reynolds number for one configuration. The three sets

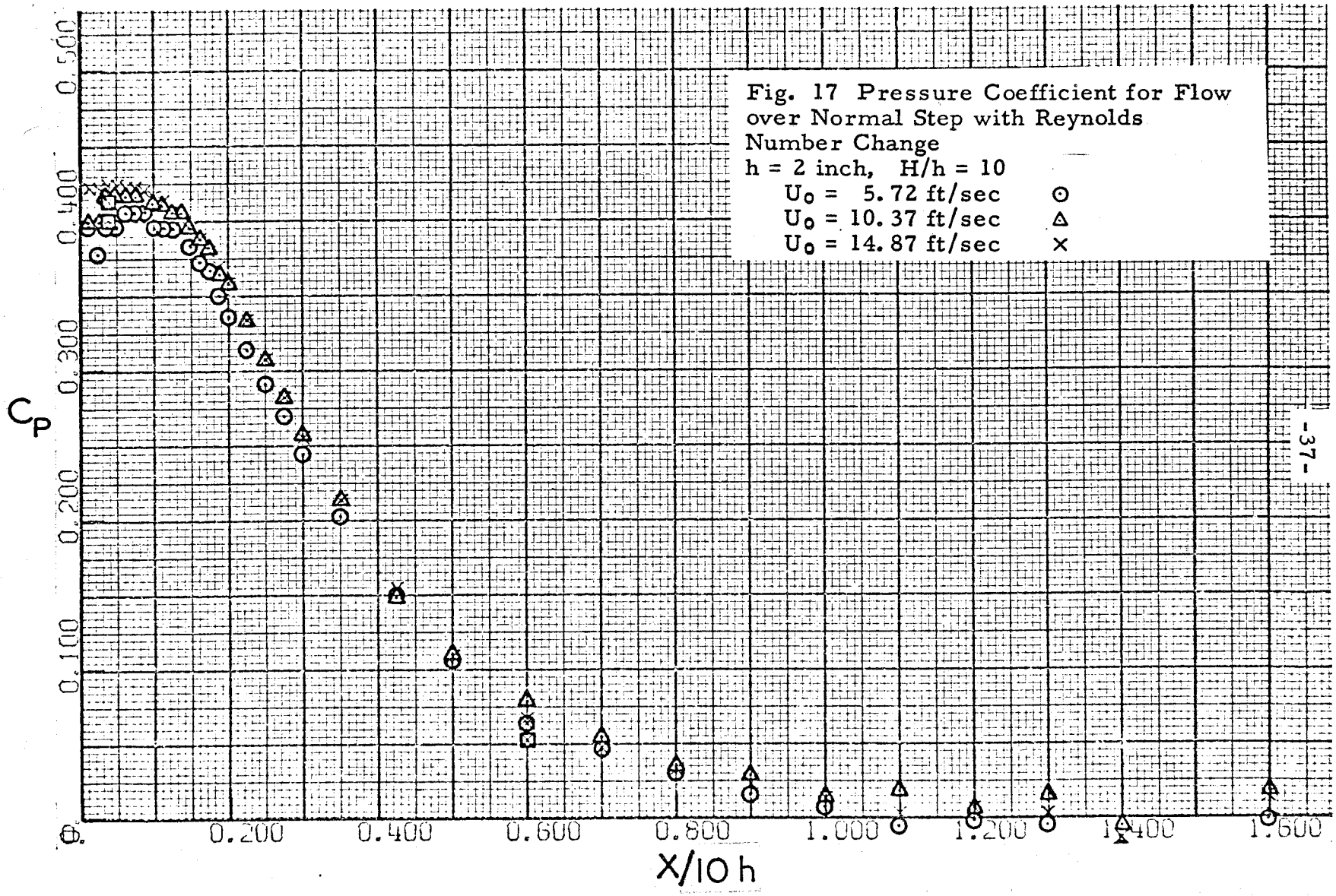
Fig. 17 Pressure Coefficient for Flow over Normal Step with Reynolds Number Change
h = 2 inch, H/h = 10
U_o = 5.72 ft/sec ⊙
U_o = 10.37 ft/sec △
U_o = 14.87 ft/sec ×
C_p
0.500
0.400
0.300
0.200
0.100
0
0.200
0.400
0.600
0.800
1.000
1.200
1.400
1.600
X/10 h

of data represent a Re or U_o change of 160 percent with insignificant change in the pressure field; the variations here are certainly within experimental accuracy. The result is typical of all configurations tested.

The effect of h/δ is shown on Figures 18 and 19. In Figure 18, blockage (H/h) is held constant at $H/h = 10$, and h/δ varies from 1.0 to 2.0. For Figure 19, $H/h = 5$, and h/δ varies from 2.0 to 4.0. In all cases, the near field, i.e., x/h less than 2 or 3, is influenced significantly by the step height to boundary layer thickness ratio. Upstream of $x/h \approx 4$ or 5, the various configurations are in good agreement for fixed H/h values. There is some scatter; however, it is reasonable to say that the influence of h/δ does not affect the far upstream pressure field.

In order to demonstrate the effects of the external geometry on the pressure field, Figures 20, 21, and 22 are presented, which show data for varying H/h with h/δ held fixed. The circled data and the crossed data on Figure 20 show a change from $H/h = 10$ to $H/h = 20$, respectively, with $h/\delta = 1.0$, and the triangle data again indicate the effect of a change in h/δ with $H/h = 10$. Figure 21 shows a blockage change from $H/h = 5$ for the crossed data to $H/h = 10$ for the circled data, with h/δ remaining constant at 2.0. As the interference of the step is decreased (H/h becoming larger) for h/δ constant, the step influence moves farther upstream, in terms of step heights, and affects the far upstream pressure field; the effect on the near field is less significant.

The effects of blockage and h/δ changes are summarized in

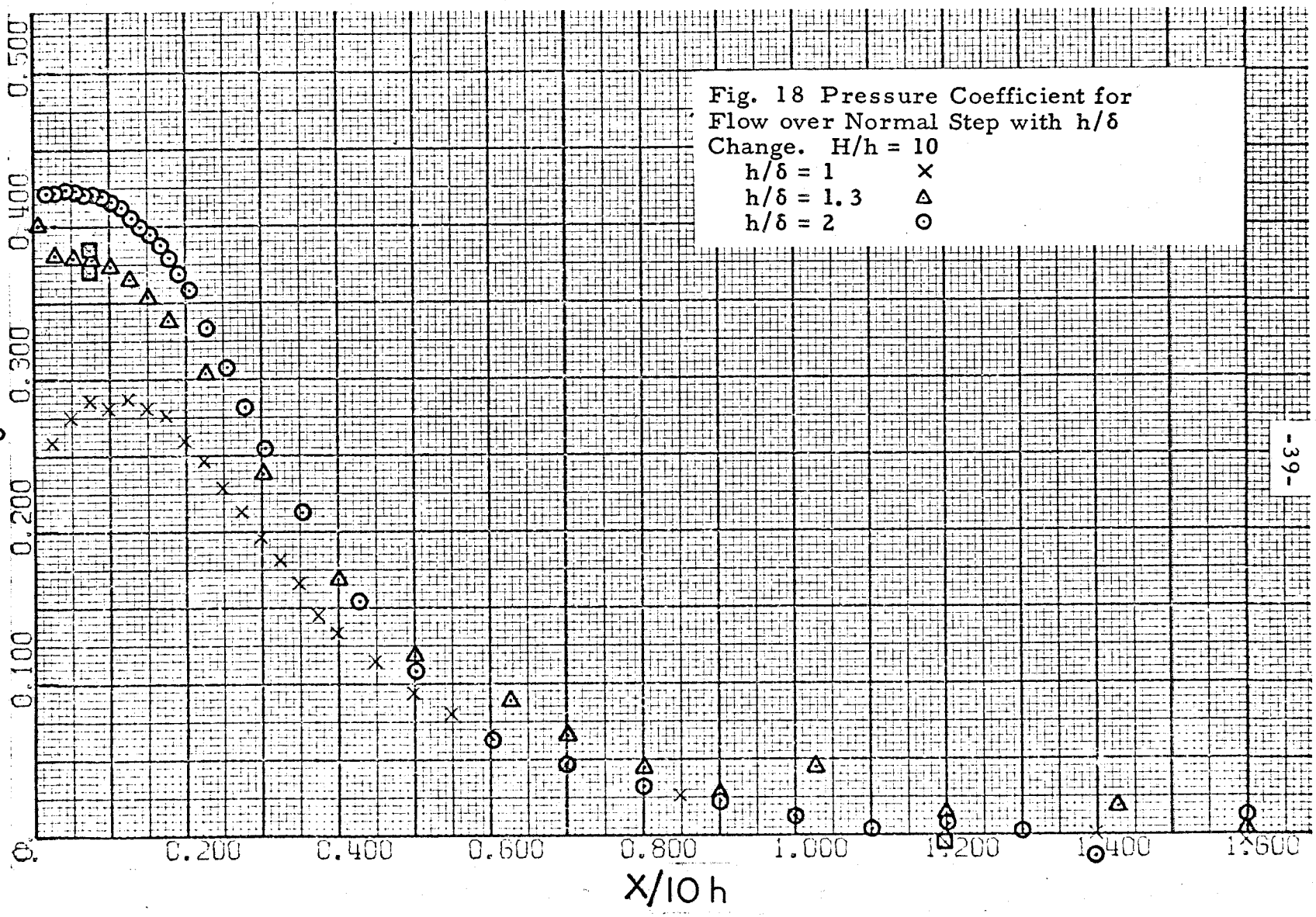
Fig. 18 Pressure Coefficient for Flow over Normal Step with h/δ Change. H/h = 10
h/δ = 1 ×
h/δ = 1.3 △
h/δ = 2 ⊙
Cp
0.500
0.400
0.300
0.200
0.100
0.
0.200
0.400
0.600
0.800
1.000
1.200
1.400
1.600
X/10 h

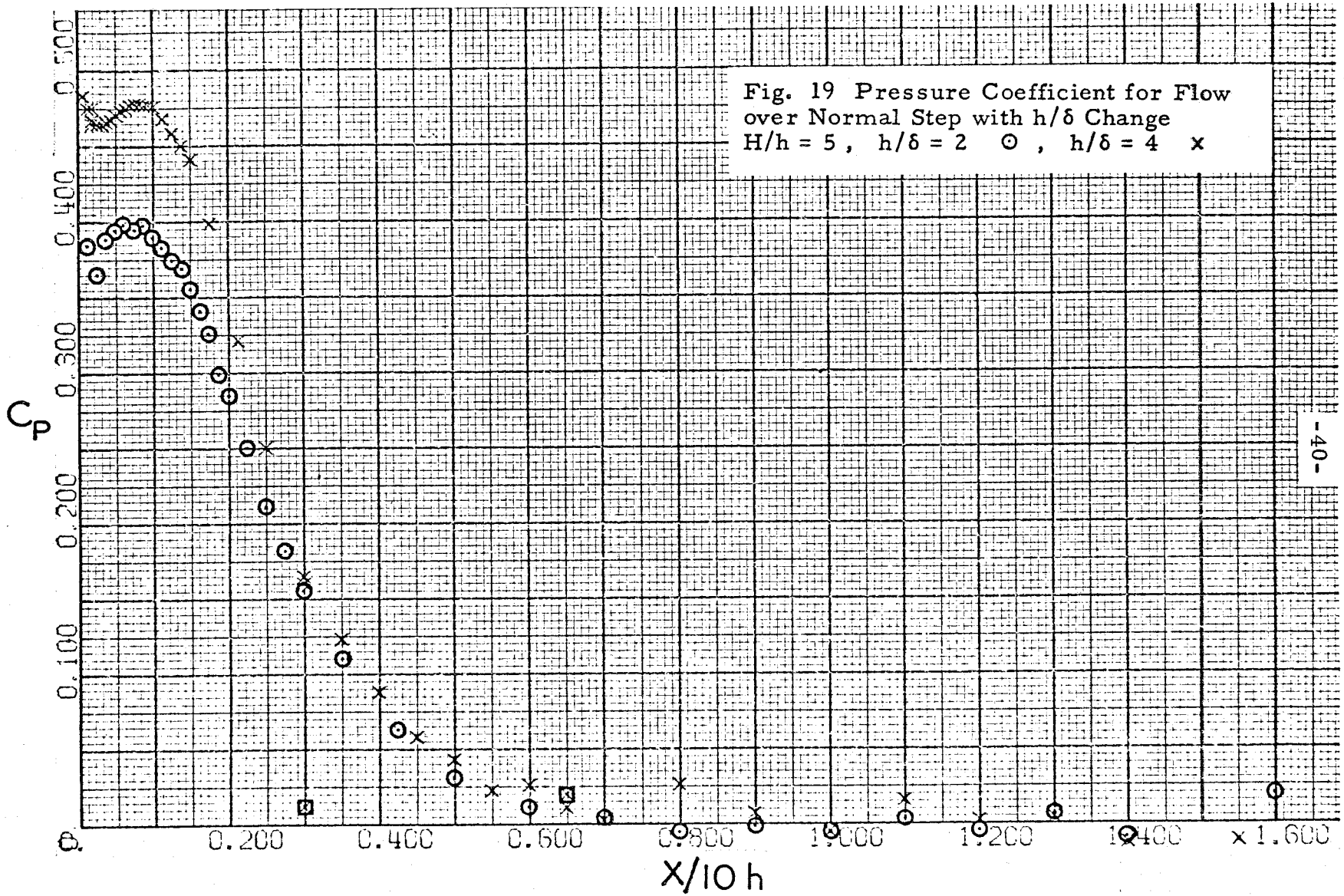

Fig. 19 Pressure Coefficient for Flow over Normal Step with h/δ Change
H/h = 5 , h/δ = 2 ⊙ , h/δ = 4 x

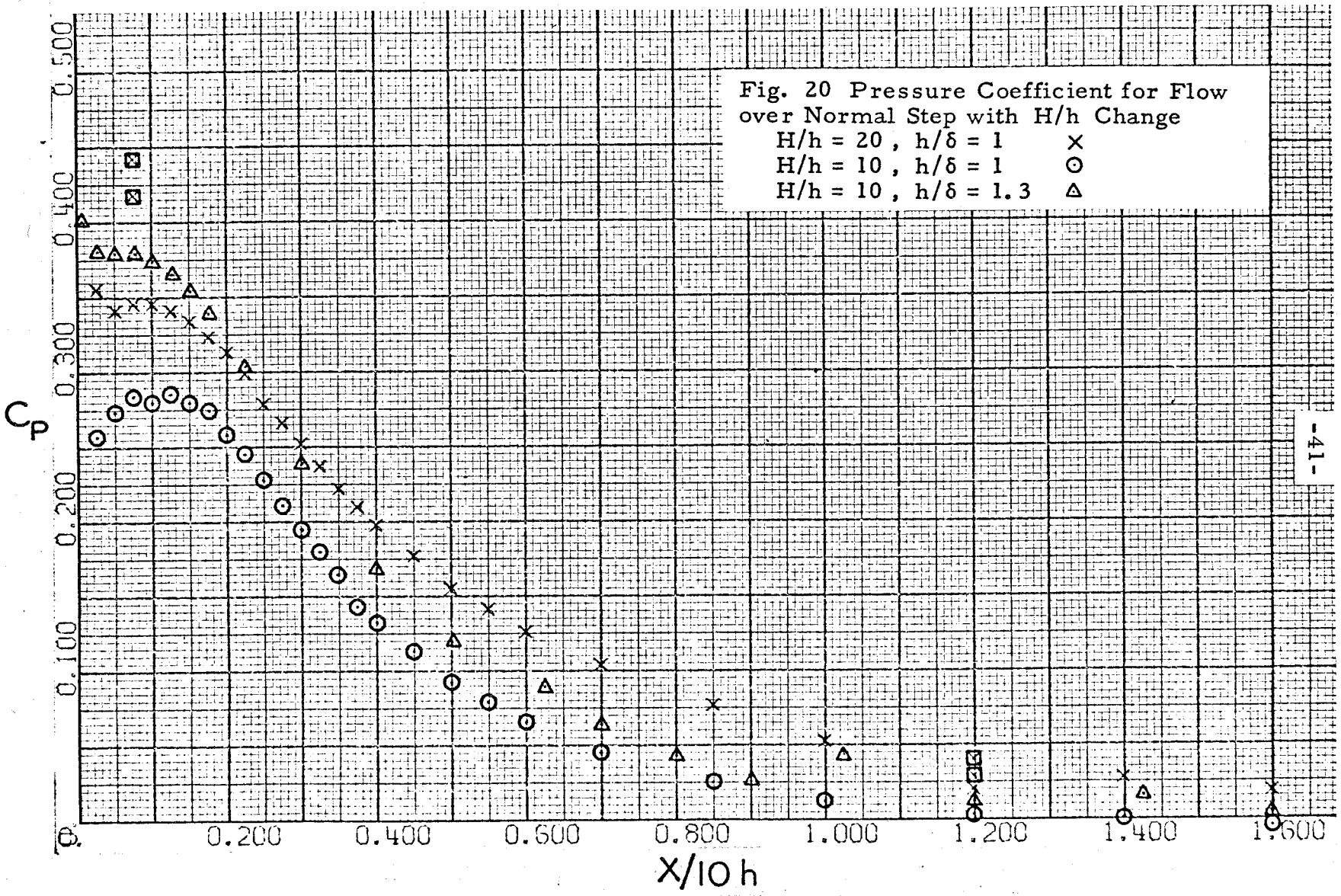
Fig. 20 Pressure Coefficient for Flow over Normal Step with H/h Change
H/h = 20 , h/δ = 1
H/h = 10 , h/δ = 1
H/h = 10 , h/δ = 1.3
Cp
0.500
0.400
0.300
0.200
0.100
0
0.200
0.400
0.600
0.800
1.000
1.200
1.400
1.600
X/10 h

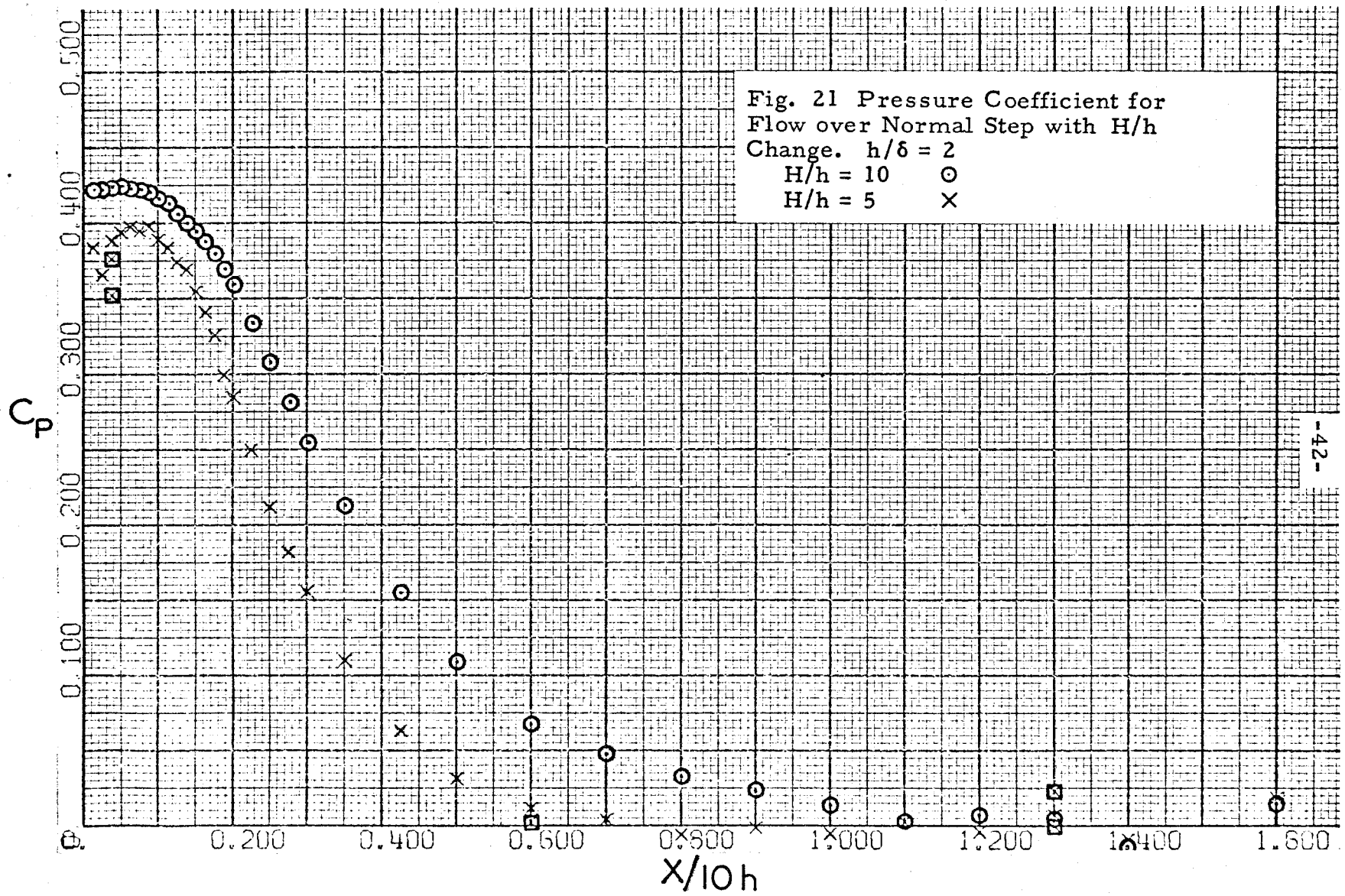

Fig. 21 Pressure Coefficient for Flow over Normal Step with H/h Change. $h/\delta = 2$
$H/h = 10$ ⊙
$H/h = 5$ ×

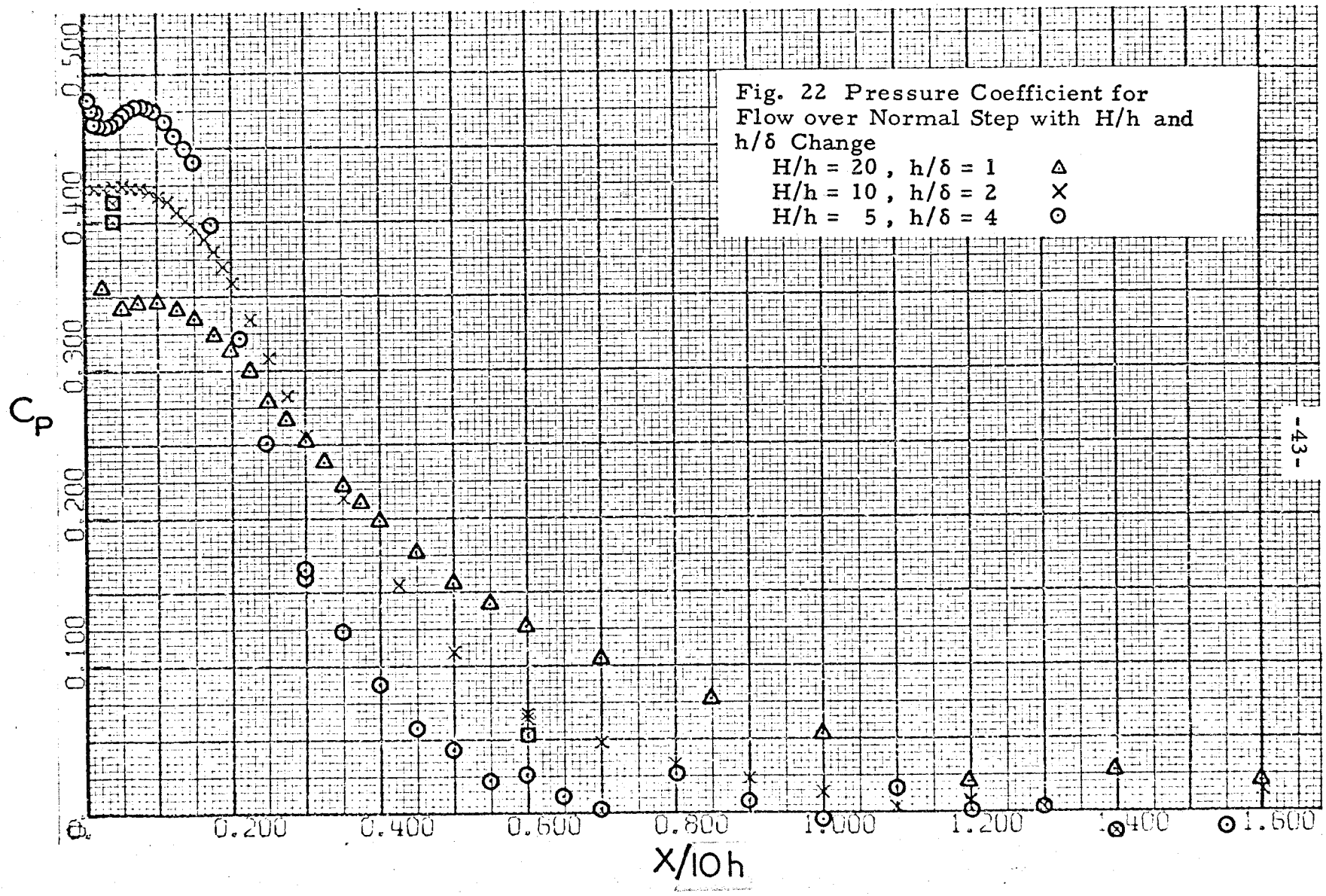
Fig. 22 Pressure Coefficient for Flow over Normal Step with H/h and h/δ Change
H/h = 20 , h/δ = 1 △
H/h = 10 , h/δ = 2 ×
H/h = 5 , h/δ = 4 ⊙
Cp
0.500
0.400
0.300
0.200
0.100
0
0.200
0.400
0.600
0.800
1.000
1.200
1.400
1.600
X/10h

Figure 22. The triangle data represent $H/h = 20$ and $h/\delta = 1$; the crossed data represent $H/h = 10$ and $h/\delta = 2$; and the circled data represent $H/h = 5$ and $h/\delta = 4$. Note that the far upstream pressure field is governed by the external flow geometry and that the upstream influence (in terms of step heights) varies inversely as the blockage. But as the near field ($x/h < 3$) is approached, the boundary layer interaction becomes dominant and controls the near-field pressure level.

The influence of h/δ on the near-field pressure level has been demonstrated above, but is more clearly demonstrated in Figure 23 where the effect of h/δ on the maximum pressure coefficient is shown. The value selected as the maximum pressure coefficient is the peak value for the plateau region close to the step base but not in the recirculating region very near the corner where step and flat plate meet. This value is close to, but larger than, the separation pressure coefficient. Note in Figure 23 that as the h/δ ratio increases, the maximum pressure also increases, but that the influence of a H/h change does not significantly change the maximum values. (The flagged symbols in Figure 23 indicate a change in blockage by a factor of two by use of image steps but with no change in h/δ.) Estimated maximum pressure coefficients of Bradshaw[1], Taulbee[2], and Chapman, et al.[3], obtained by a data reduction technique similar to that used here, are also shown, and these are in good agreement with the present data. The value of maximum pressure coefficient appears to be approaching an asymptotic value of roughly 0.5 as h/δ increases above 4.

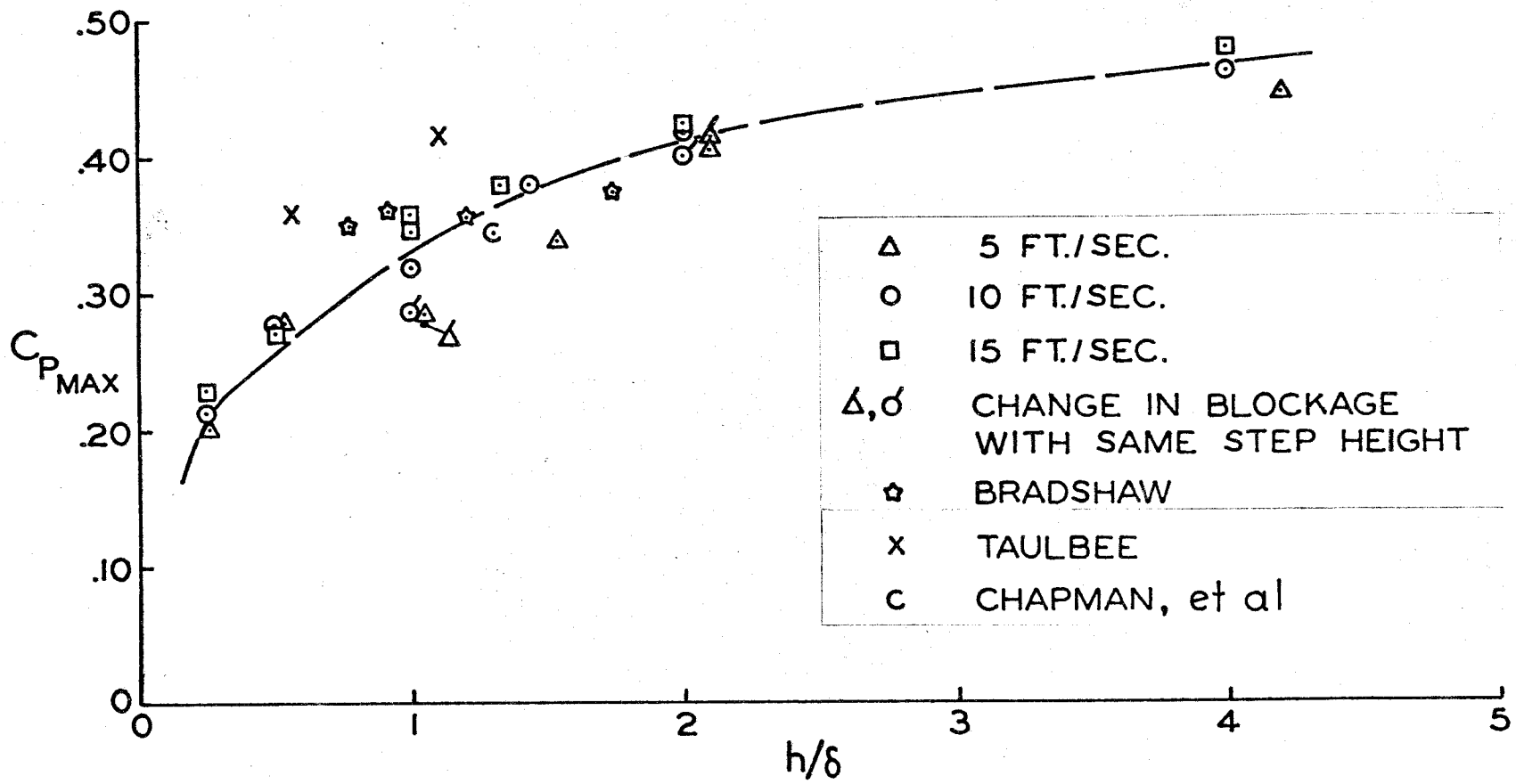

FIG. 23 VARIATION OF MAXIMUM PRESSURE COEFFICIENT

The locations of the maximum slope of the pressure coefficient curves were determined and are shown on Figure 24. This location scales approximately as twice the step height. Note that the pressure coefficient variation has an approximately linear portion near the point of maximum slope, and in picking the location of maximum slope points, the position closest to the step face was picked when any ambiguity existed. As was noticed by Bradshaw[1] and others, the separation point occurs shortly downstream of this inflection point. A few visual observations indicated a separation point of about 1.3 to 1.6 step heights in front of the step, but these observations cannot be considered accurate due to the very unsteady nature of the separation process. These estimates are to be compared with values of 1.2 reported by Bradshaw[1], 0.84 to 1.44 for the less directly applicable results of Taulbee[2], and 1.04 by Chapman, et al.[3] for a very small step.

Also, it appears that the separation point predicted by the mathematical model is at least twice as far upstream as the actual separation point. This again emphasizes the influence of h/δ on the near field flow and emphasizes the inadequacy of the mathematical model.

2. Step Face. Figures 25 through 29 show the variation of the pressure coefficient on the step face with the distance above the step base (y/h). Comparison of the data for changes in blockage and step height to boundary layer thickness showed that there is no apparent influence of these parameters on the step-face pressure field. In addition, Figure 30 presents data for the h = 2 inches configuration

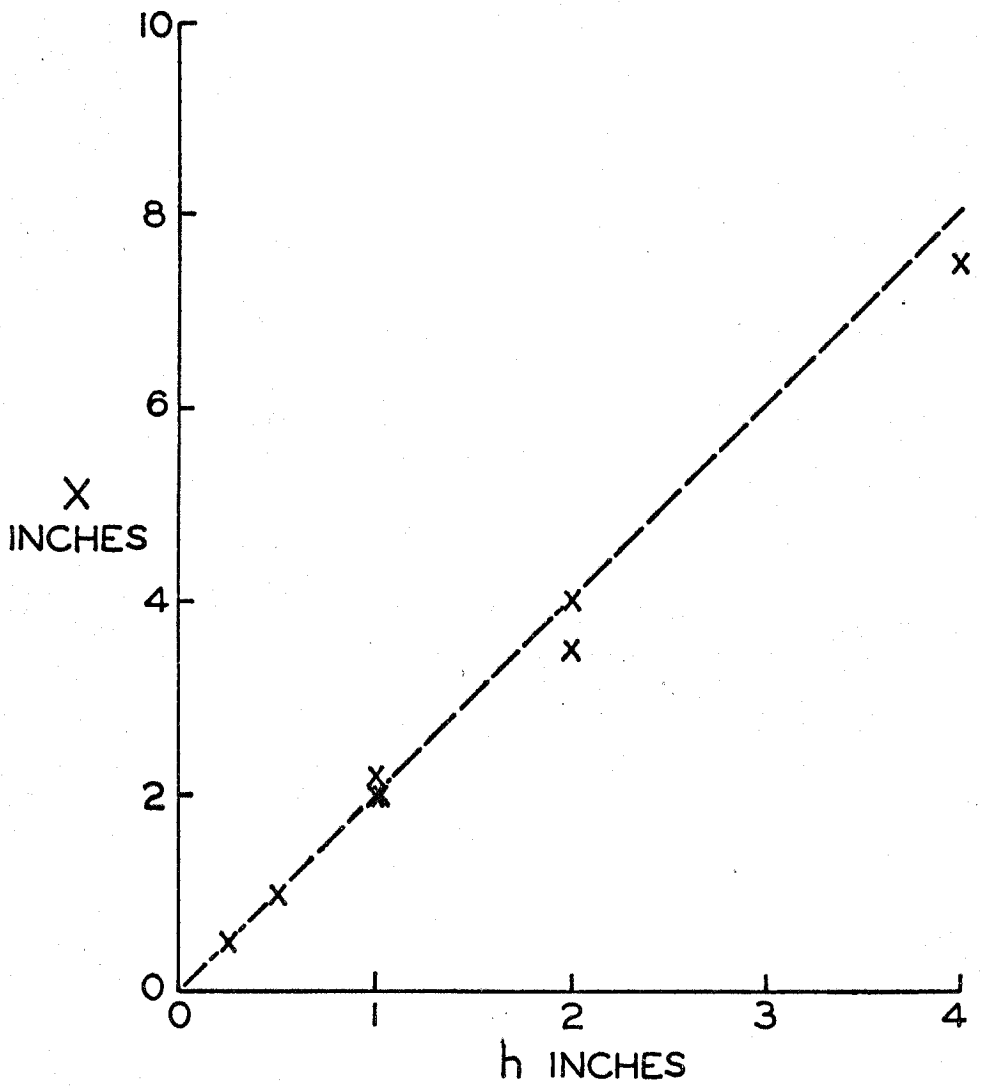

FIG. 24 LOCATION OF MAXIMUM CHANGE RATE OF PRESSURE COEFFICIENT FOR FLOW OVER NORMAL STEP

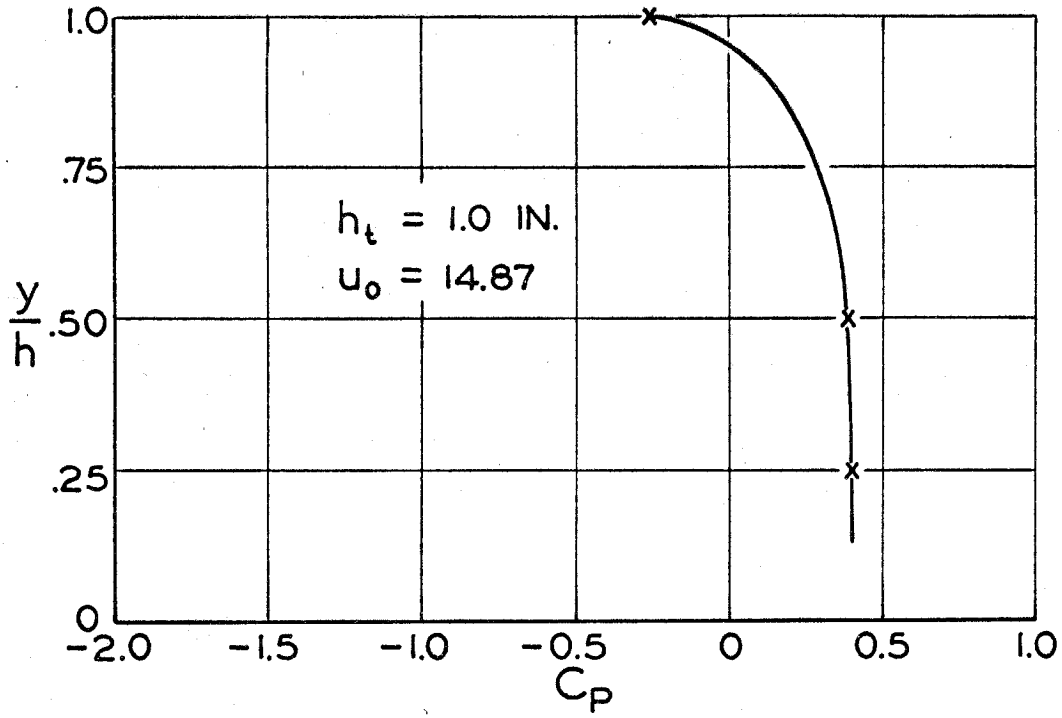

FIG. 25 PRESSURE COEFFICIENT ON STEP FACE

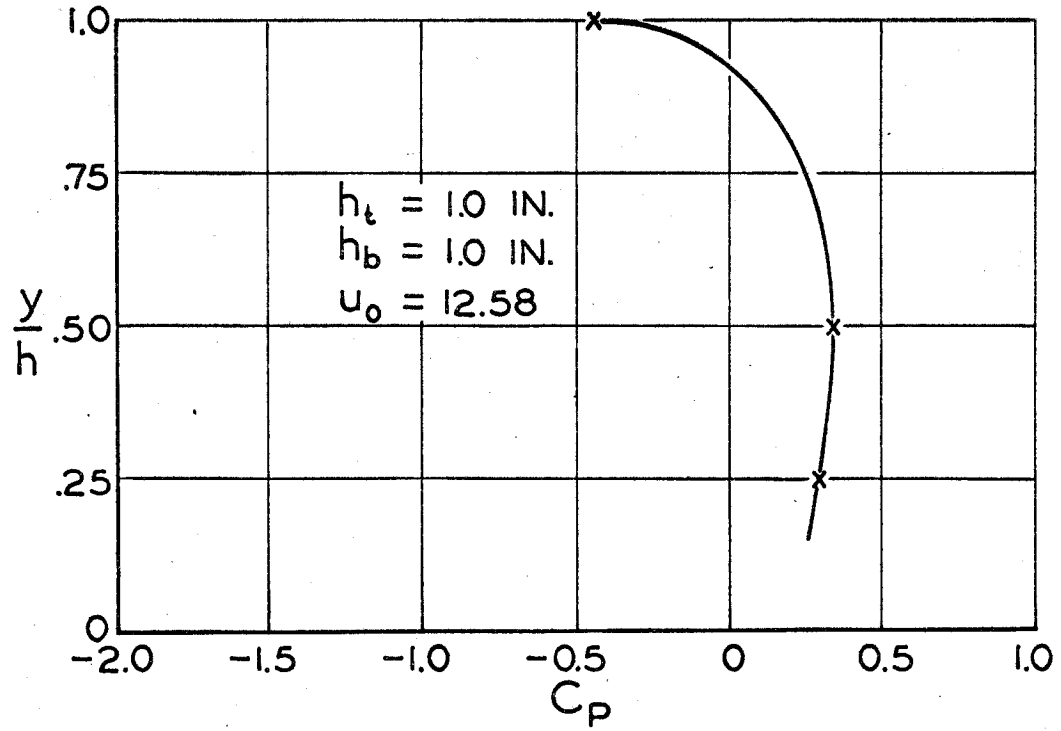

FIG. 26 PRESSURE COEFFICIENT ON STEP FACE

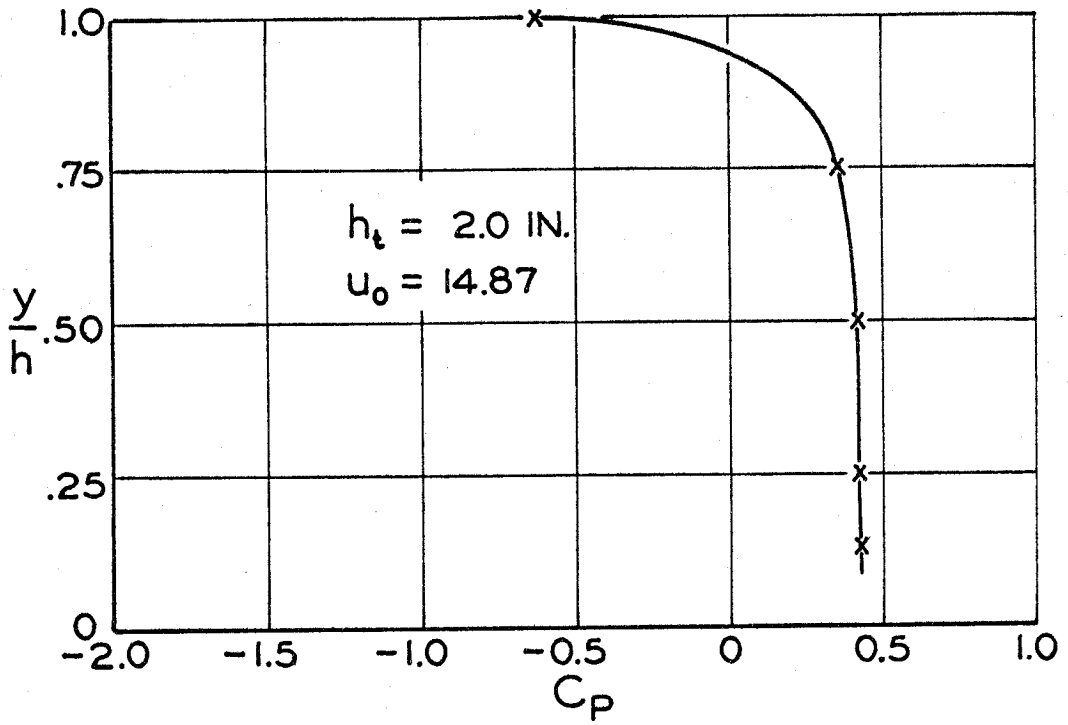

FIG. 27 PRESSURE COEFFICIENT ON STEP FACE

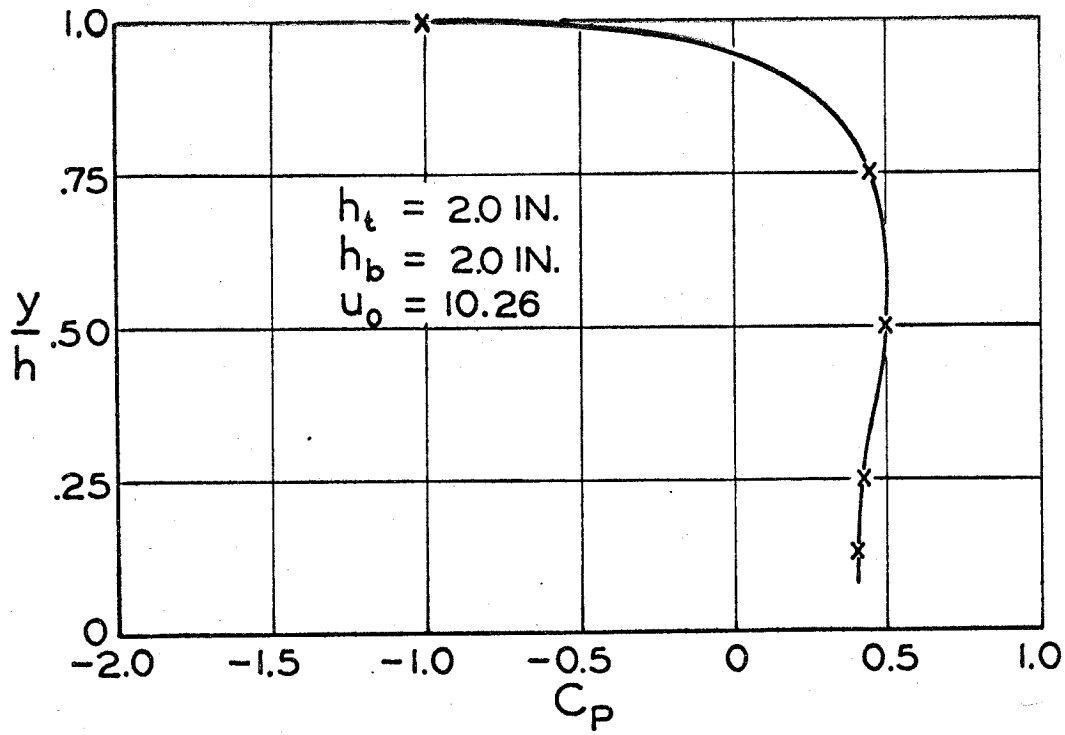

FIG. 28 PRESSURE COEFFICIENT ON STEP FACE

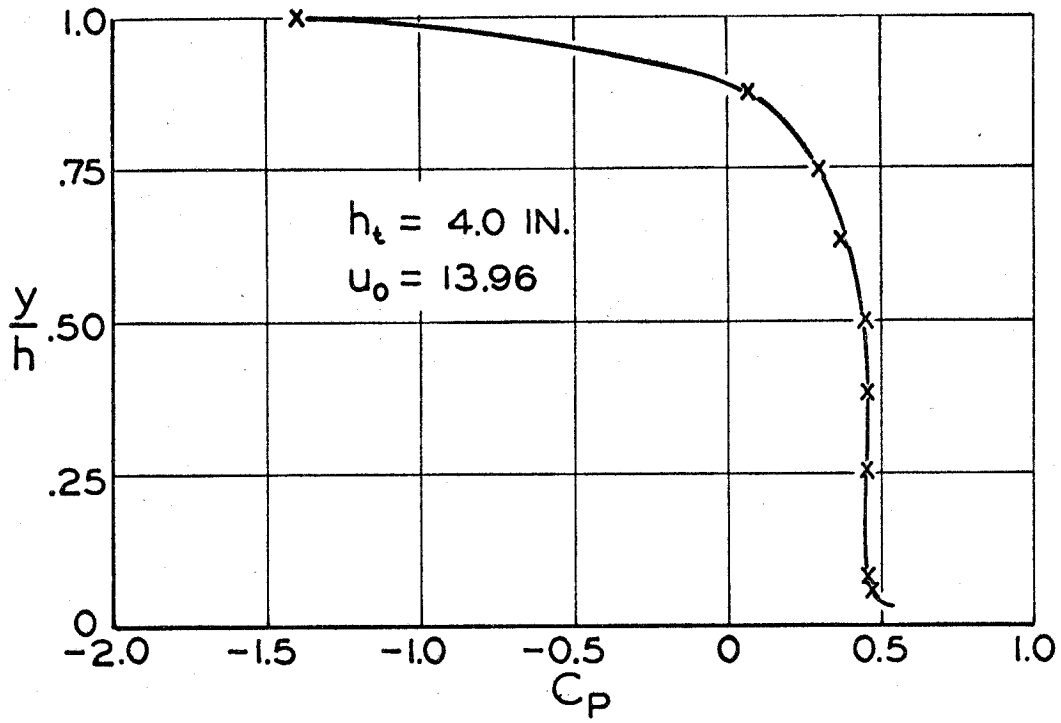

FIG. 29 PRESSURE COEFFICIENT ON STEP FACE

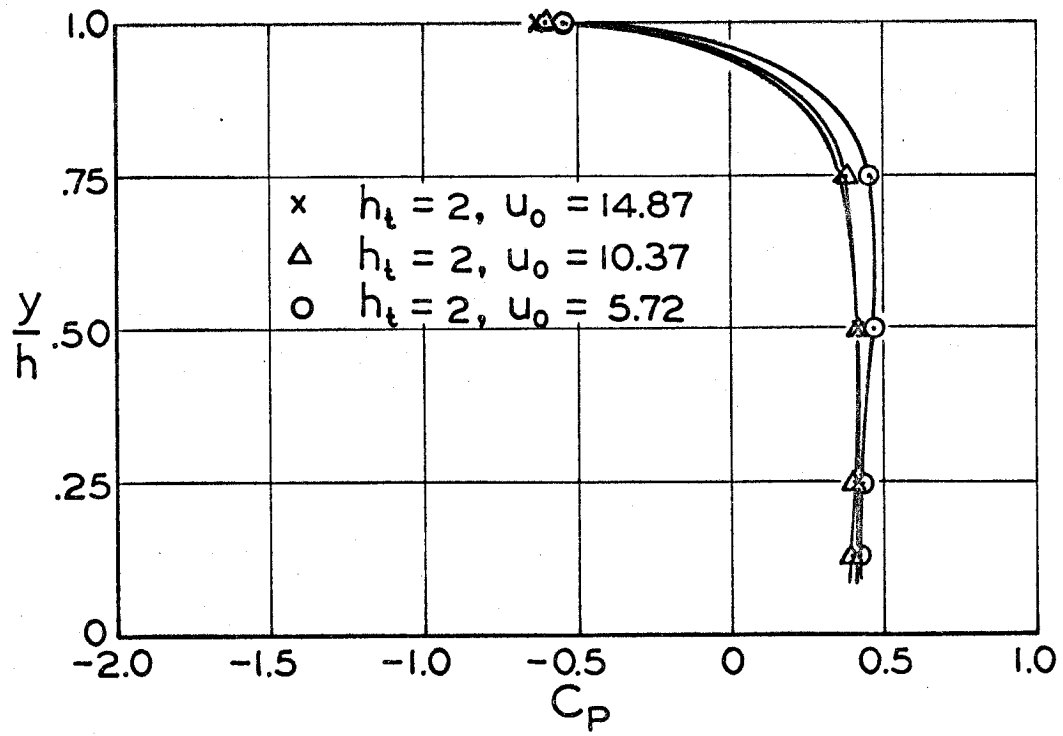

FIG. 30 PRESSURE COEFFICIENT ON STEP FACE

for each of the three tunnel speeds used, and these data show that there is no significant Reynolds number effect.

From these figures it is seen that the pressure gradient is roughly zero up to about $y/h = 0.5$, at which point the pressure coefficient decreases rapidly as the flow approaches the sharp edge of the step top. This, of course, suggests that the flow reattaches at about $y/h = 0.5$, and this value is consistent with Taulbee's[2] observation of $y/h = 0.6$. Further visual observations also showed that the reattachment point was near $y/h = 0.5$; however, the location of the reattachment point is very unsteady as judged from visual observation of dye and air injectants. In contrast, calculations performed using the mathematical model show that the reattachment point is at the top of the step face with the pressure coefficient staying constant at the separation value.

Table IV shows the comparison of the maximum pressure coefficient in front of the step with the maximum pressure coefficient on the step face. Differences vary from 0 to 22 percent, and with the exception of the 4-inch step, the pressure coefficient on the step face was higher than in front of the step. There does exist a reversed circulatory region very near the step base, at which point the pressure coefficient is higher than the upstream value near separation. There was only one configuration with a wall pressure tap at the corner which was close enough to the step base to accurately reflect this region, and it did show that the two pressure coefficients were the same.

3. Top of Step. Figures 31 through 35 present the variation of pressure coefficient with downstream location, where (-x) repre-

Step Height (inches)	U_o (ft/sec)	$C_{P_{max}}$ in front of step	$C_{P_{max}}$ on step face
$h_t = 1$	14.87	.35	.39
$h_t=1$, $h_b=1$	12.58	.28	.34
$h_t = 2$	14.87	.42	.42
$h_t=2$, $h_b=2$	10.26	.40	.49
$h_t = 4$	13.96	.48	.46

TABLE IV. MAXIMUM PRESSURE COEFFICIENT IN FRONT OF STEP AND ON STEP FACE

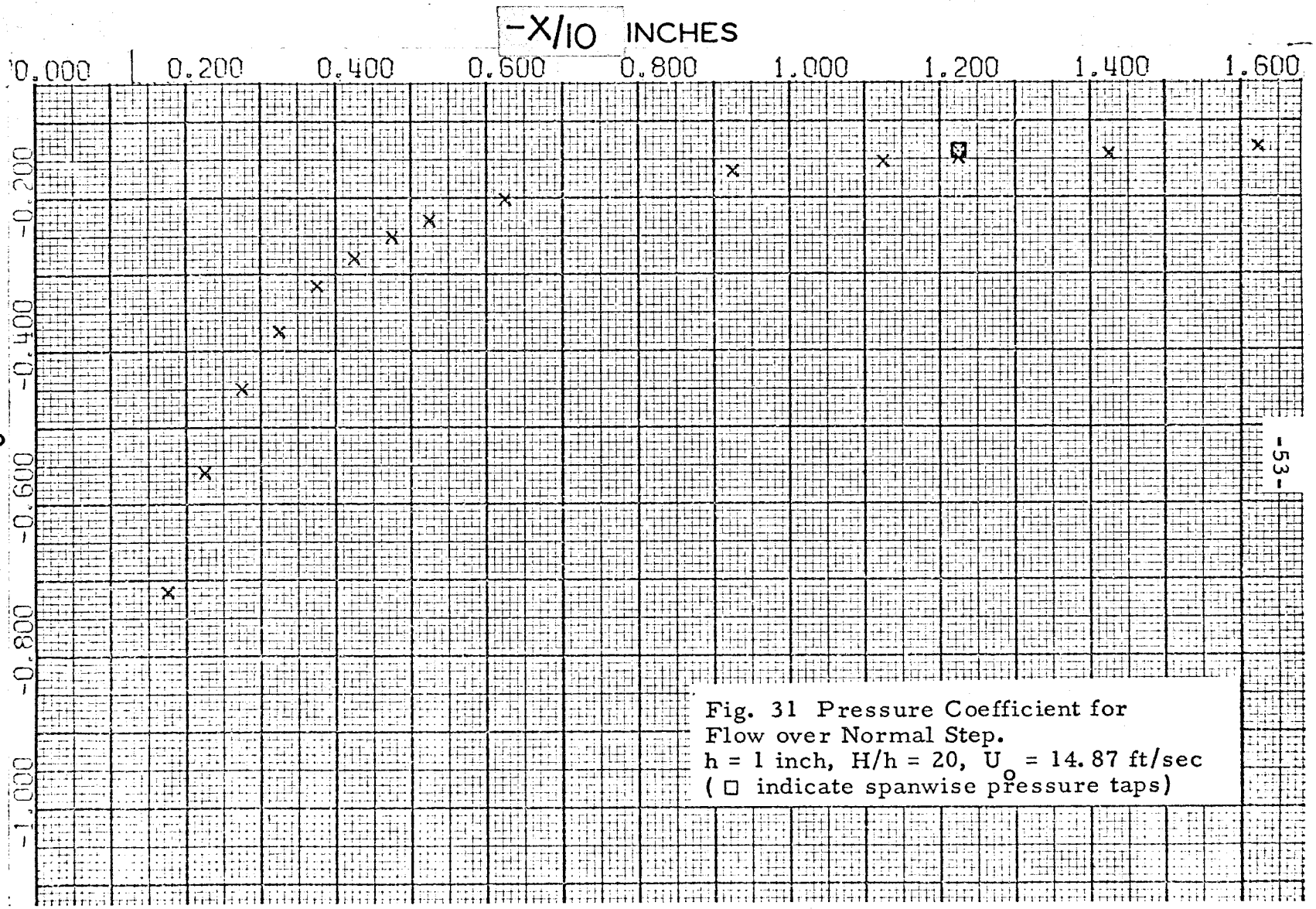

Fig. 31 Pressure Coefficient for Flow over Normal Step.
h = 1 inch, H/h = 20, U_o = 14.87 ft/sec
(□ indicate spanwise pressure taps)

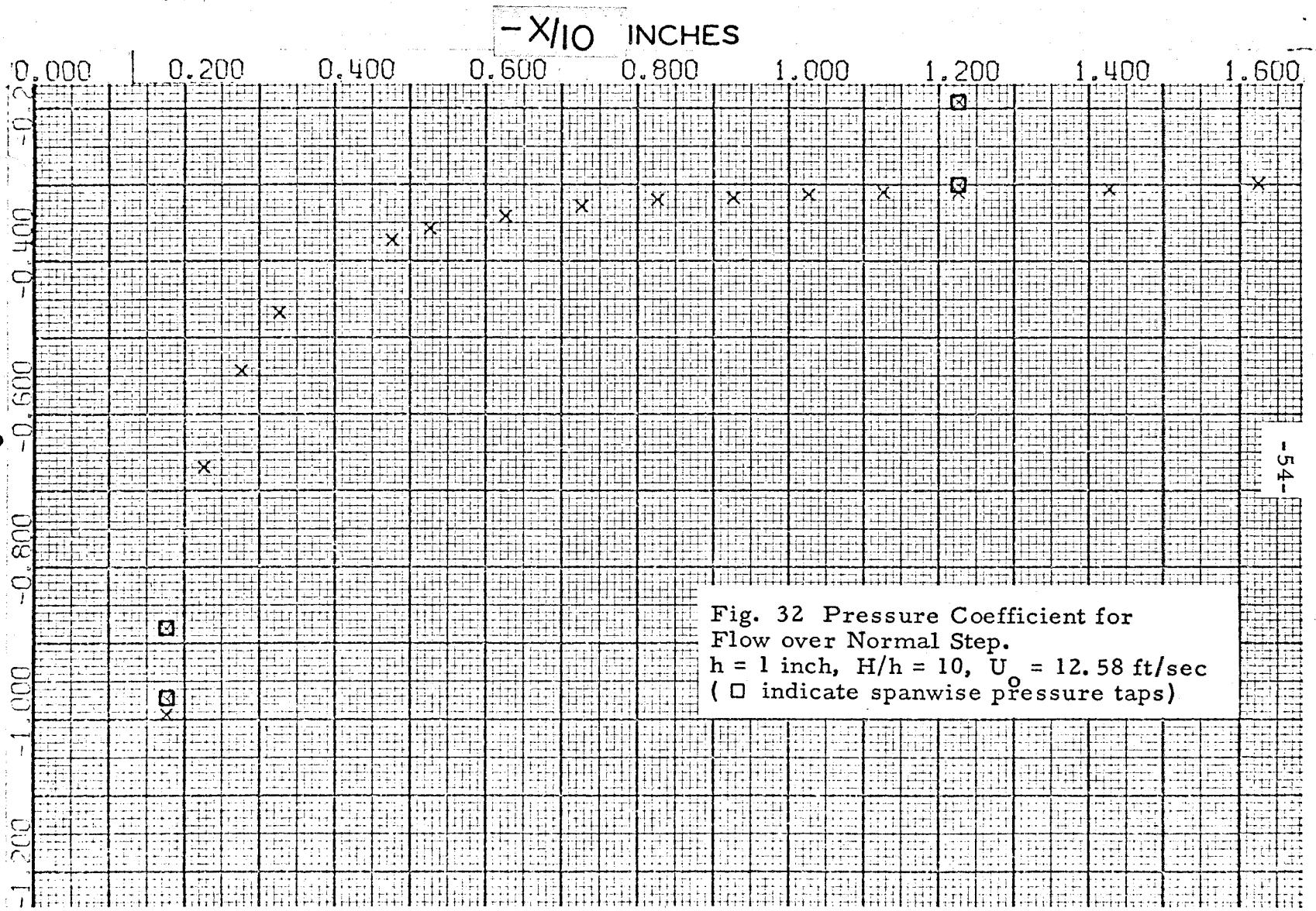

Fig. 32 Pressure Coefficient for Flow over Normal Step.
h = 1 inch, H/h = 10, U_o = 12.58 ft/sec
(□ indicate spanwise pressure taps)

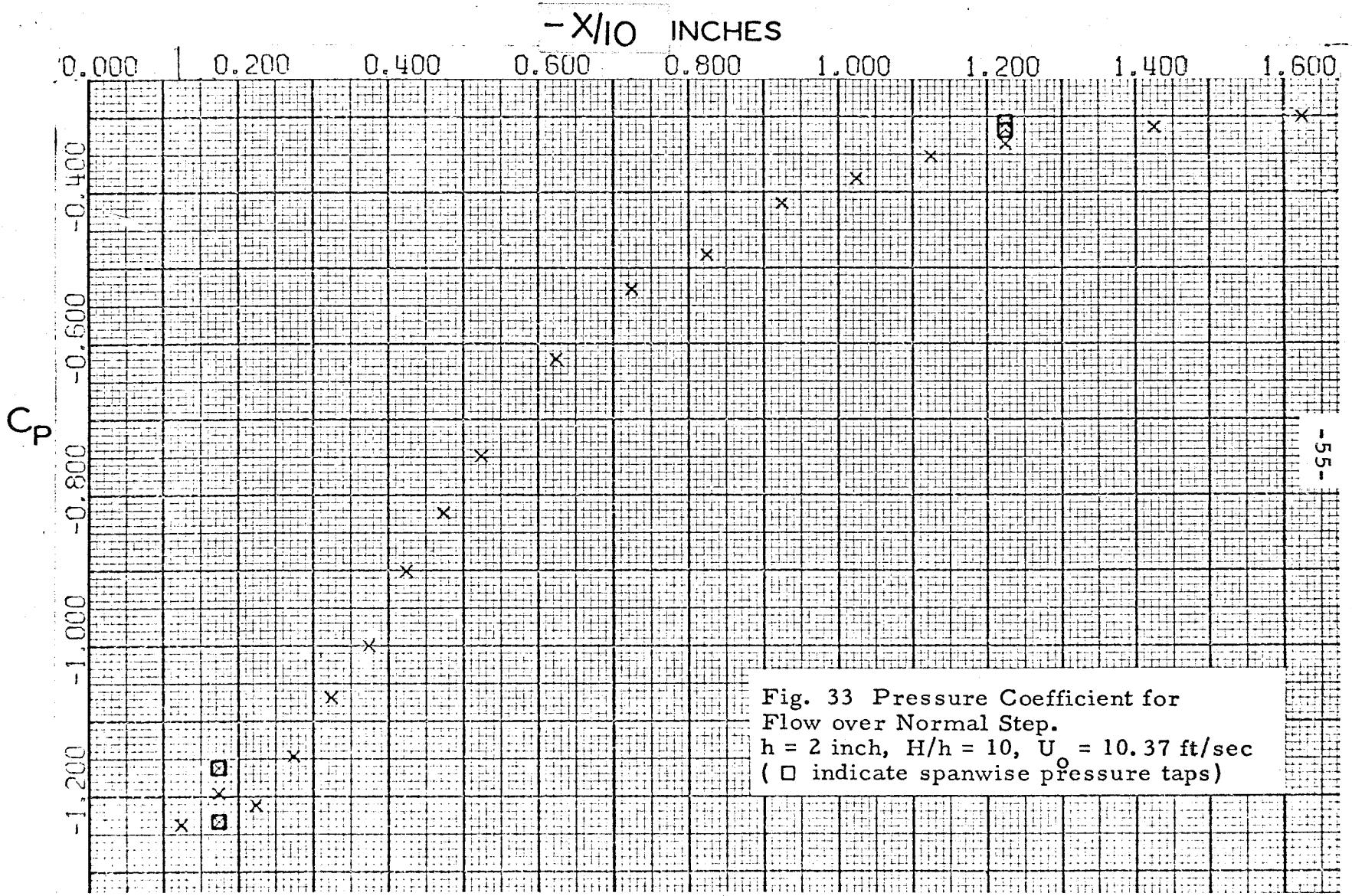

Fig. 33 Pressure Coefficient for Flow over Normal Step.
h = 2 inch, H/h = 10, U_o = 10.37 ft/sec
(□ indicate spanwise pressure taps)

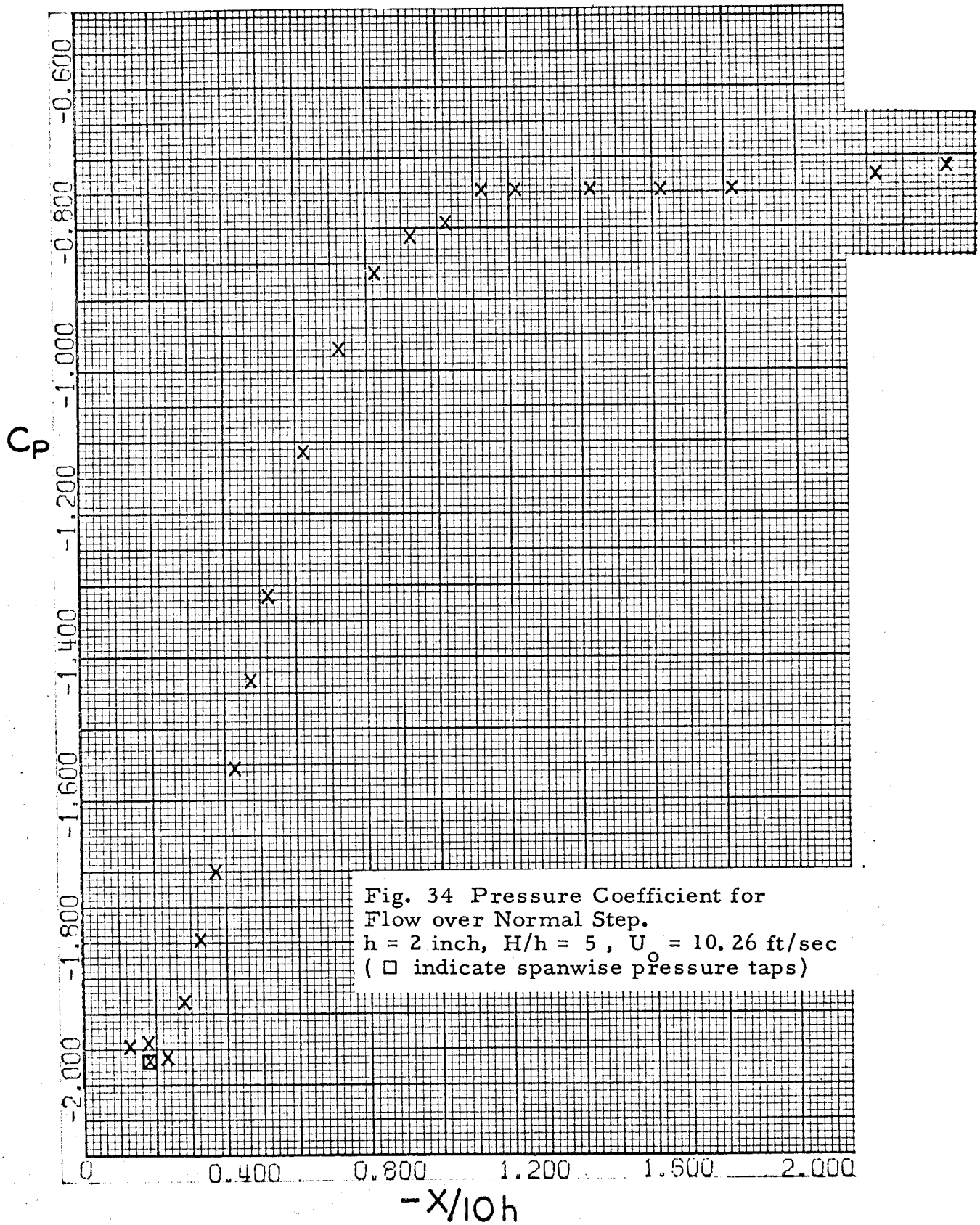

Fig. 34 Pressure Coefficient for Flow over Normal Step.
h = 2 inch, H/h = 5 , U_o = 10.26 ft/sec
(□ indicate spanwise pressure taps)

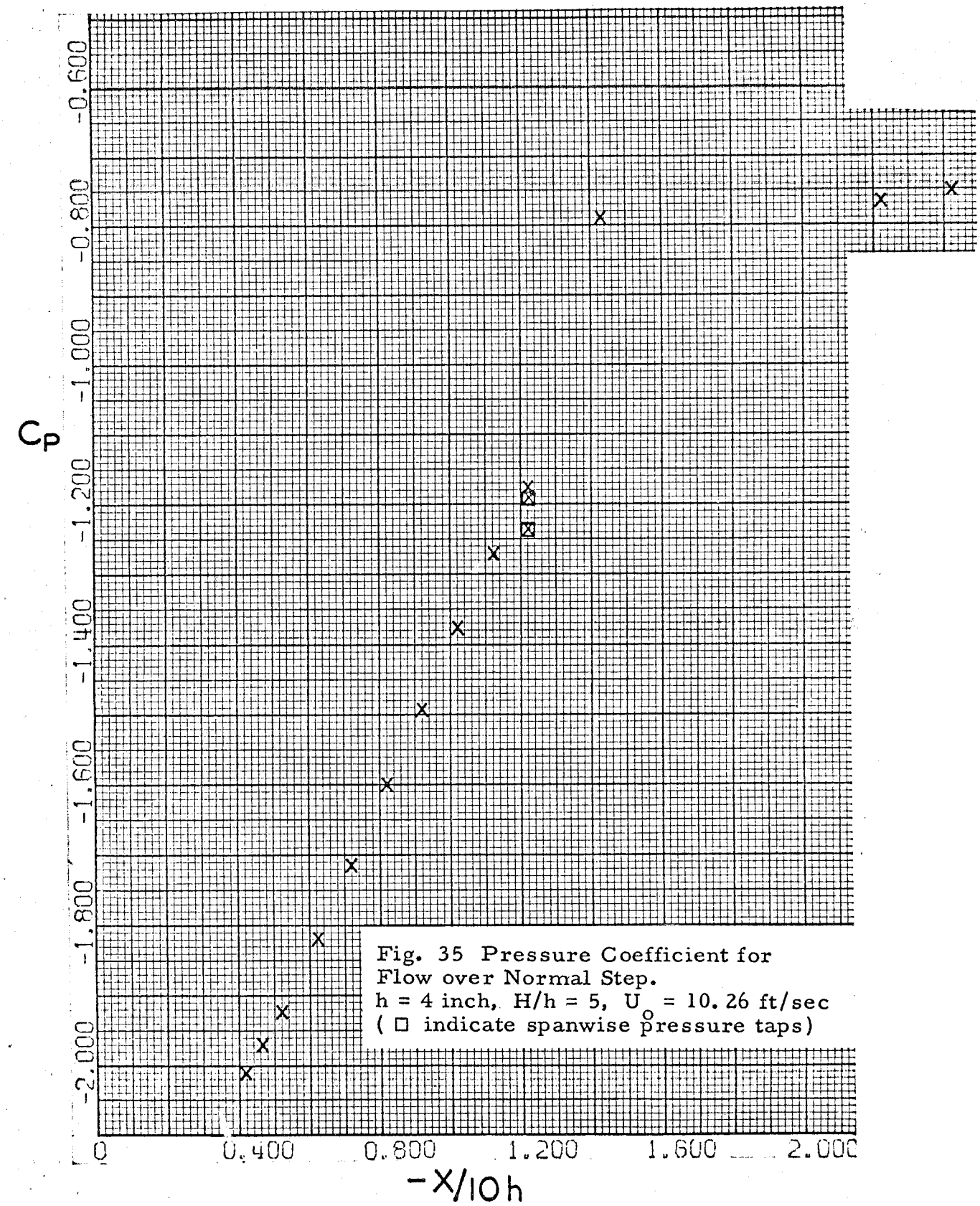

Fig. 35 Pressure Coefficient for Flow over Normal Step.
h = 4 inch, H/h = 5, U_o = 10.26 ft/sec
(□ indicate spanwise pressure taps)

sents the distance measured downstream from the leading edge of the step. Due to limitations in the manometer set-up, some of the more negative pressure readings were not collected; hence, some data points close to the leading edge of the step are not presented. No pressure data were taken for the 1/4-inch and 1/2-inch step heights. There were two sets of spanwise pressure taps on top of the step, and these data are indicated by the blocked points. For the larger step heights, the differences between centerline and off-axis pressures decreased, and hence the two-dimensionality on top of the step probably becomes much better. This is commensurate with the behavior of the regions upstream of the step.

Computations were performed using the mathematical model described in Section III which describe the dividing streamline for the dead water region on top of the step. The geometry of the liquid cavity was made visible by injection of air upstream of the step face; the resulting gas bubbles were swept over the step and cavity and gave a rough outline of the cavity which could be photographed. Figure 36 shows the comparison of the actual cavity and the theoretical cavity; the theoretical region is shown as a solid curve with the actual test results as points. This comparison of the actual liquid cavity with the mathematical model indicates that the actual recirculating region is not as high as the mathematical model would predict. The actual layer seems to level off and maintain a fixed height, highly turbulent, mixing region far downstream.

Figures 36d and 36e indicate the extremely good agreement of the cavity shapes when the actual flow region was a gas cavity. Again,

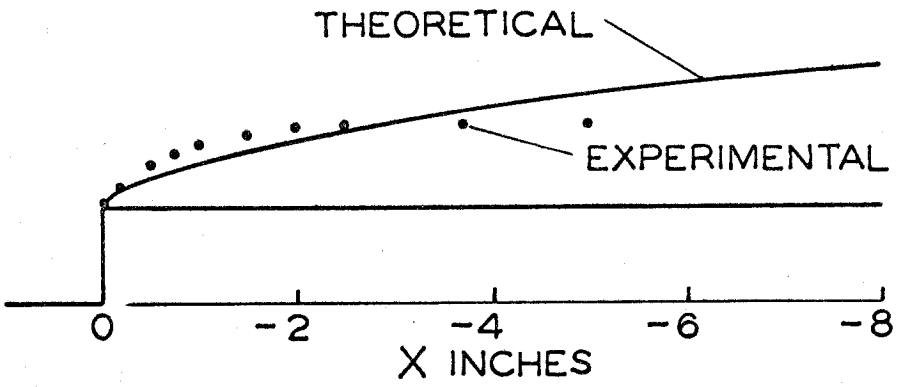

(a) h_t = 1 INCH, U_o = 14.87 FT/SEC

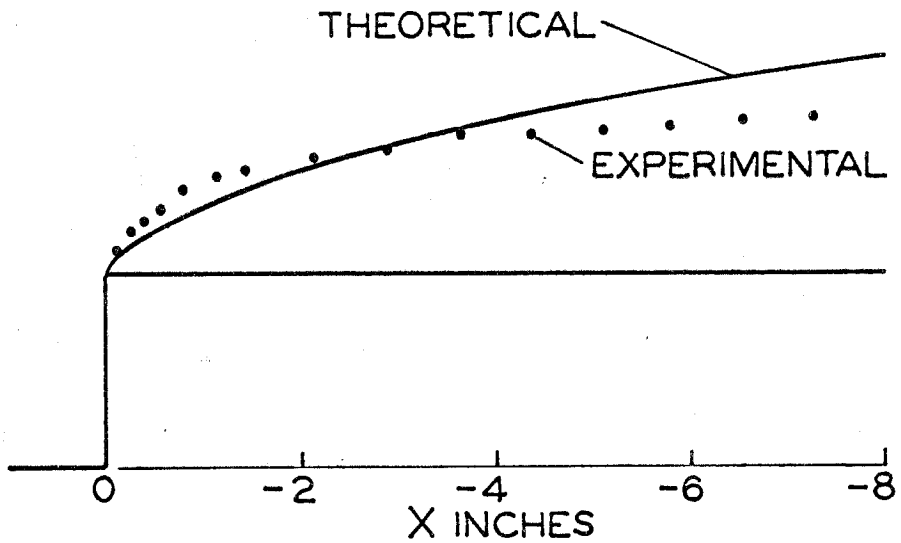

(b) h_t = 2 INCHES, U_o = 14.87 FT/SEC

FIG. 36 DIVIDING STREAMLINE FOR CAVITATING FLOW OVER NORMAL STEP COMPARED WITH ACTUAL FLOW

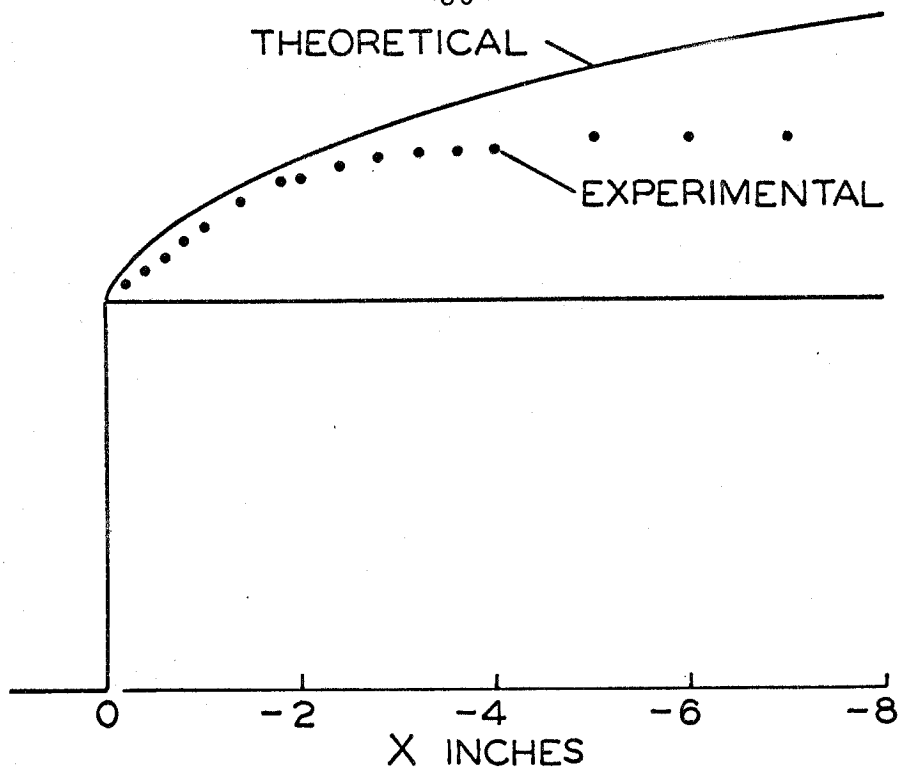

(c) h_t = 4 INCHES, U_o = 13.96 FT/SEC

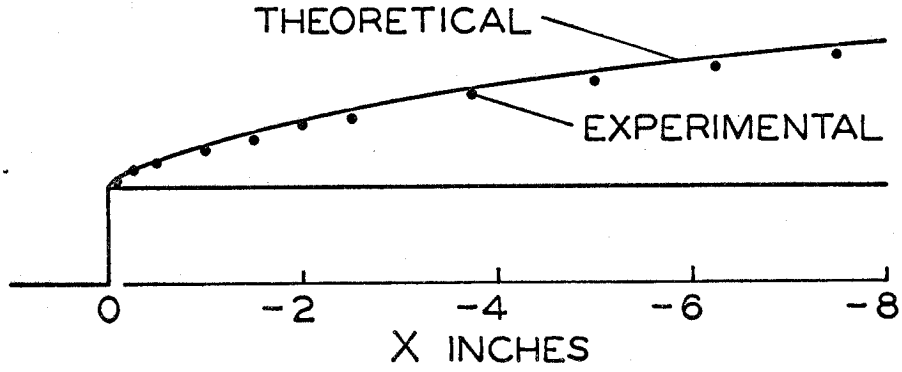

(d) h_t = 1 INCH U_o = 12.85 FT/SEC
GAS CAVITY

FIG. 36 (cont'd.) DIVIDING STREAMLINE FOR CAVITATING FLOW OVER NORMAL STEP COMPARED WITH ACTUAL FLOW

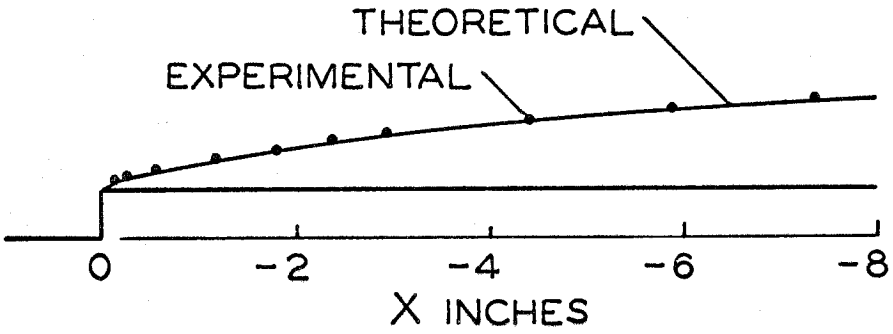

(e) h_t = .50 INCH U_o = 14.86 FT/SEC
GAS CAVITY

FIG. 36 (cont'd.) DIVIDING STREAMLINE FOR CAVITATING FLOW OVER NORMAL STEP COMPARED WITH ACTUAL FLOW

photographs were used to obtain the shape of the real cavity. As previously discussed for this case, the pressure field upstream of the step also agreed very well with the mathematical model. (It must be pointed out that the definition of the dividing streamline on the photographs is vague and that the points shown in Figure 36 are subject to some error.)

Figure 37 shows the influence of velocity or Reynolds number for one configuration. The three sets of data represent the same Reynolds number or U_o change as for the upstream region (160 percent), and again, there is no significant Reynolds number effect. These results are typical of all the velocity change data.

The effect of h/δ is shown with Figures 38 and 39. In Figure 38 the blockage is held constant at $H/h = 10$ and h/δ varies from 1.0 to 2.0. For Figure 39, $H/h = 5$ and h/δ varies from 2.0 to 4.0. Note that the pressure coefficient of the plateau region far downstream of the step is affected by a change in h/δ. However, the region near the leading edge of the step face is influenced by h/δ variations. This is best illustrated by Figure 39; here, several data points for the 4-inch step are missing since the readings were more negative than was possible to record with the manometer set-up. Even with the data available, the pressure level in the region close to the step is more negative than for the 2-inch step, indicating a direct influence of h/δ. Figure 38 indicates a like effect; here, the triangle data ($h/\delta = 1.0$) appear to level off at a less negative pressure coefficient than the crossed data ($h/\delta = 2.0$). Only three downstream data points were available for $h/\delta = 1.3$ (indicated by circled points); however, these

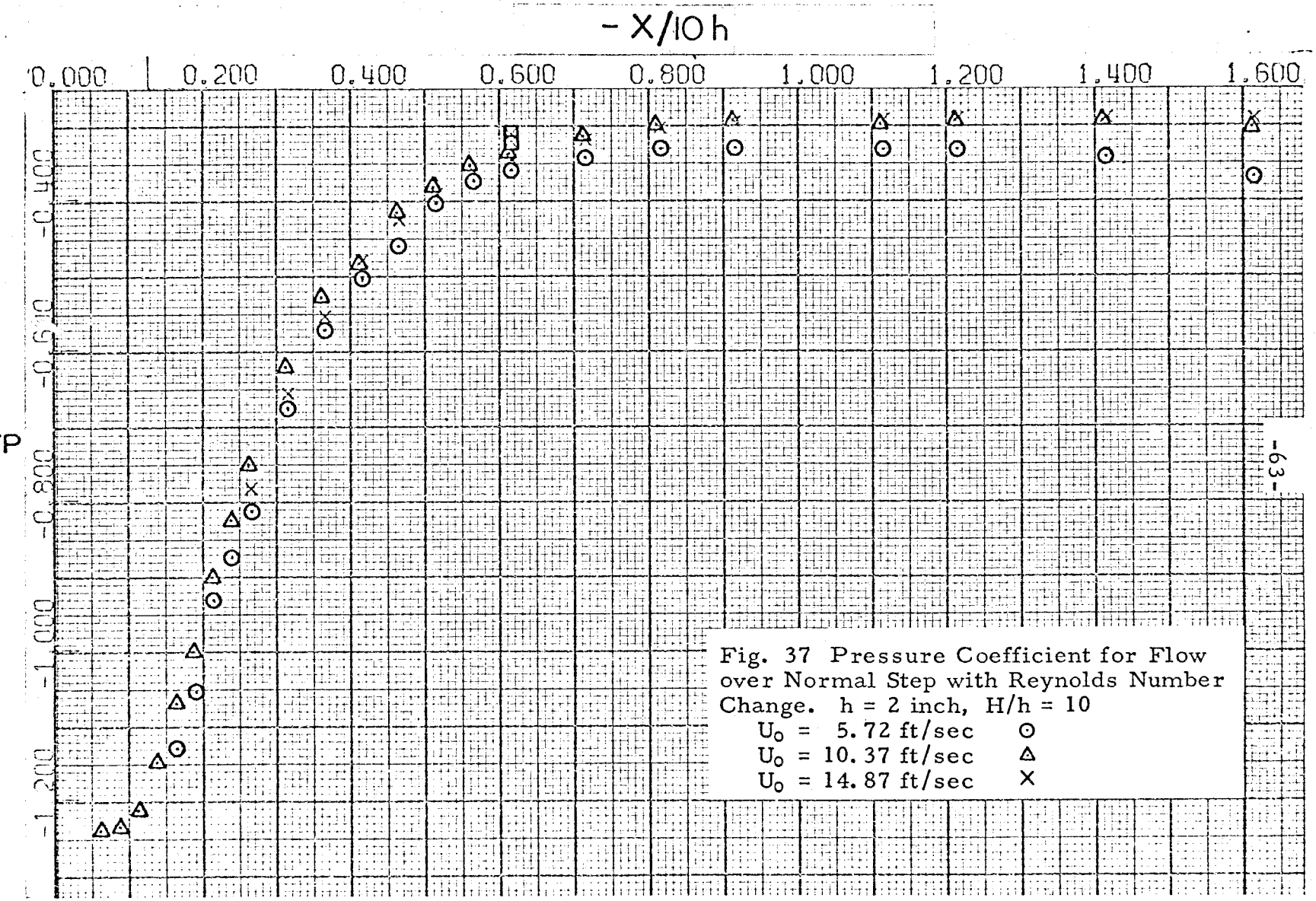

Fig. 37 Pressure Coefficient for Flow over Normal Step with Reynolds Number Change. h = 2 inch, H/h = 10

U_o = 5.72 ft/sec ⊙

U_o = 10.37 ft/sec △

U_o = 14.87 ft/sec ×

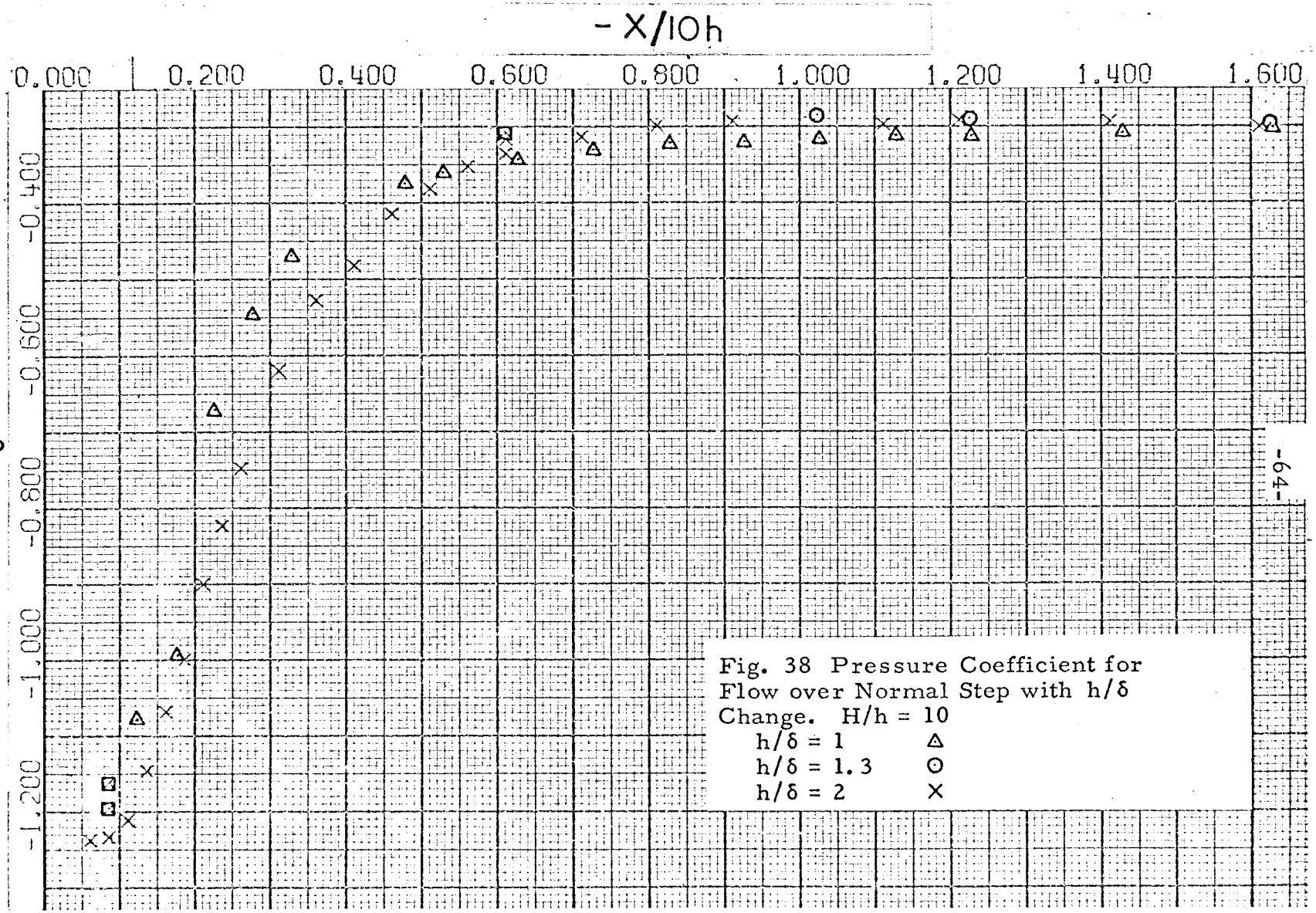

Fig. 38 Pressure Coefficient for Flow over Normal Step with h/δ Change. $H/h = 10$

$h/\delta = 1$ △

$h/\delta = 1.3$ ⊙

$h/\delta = 2$ ×

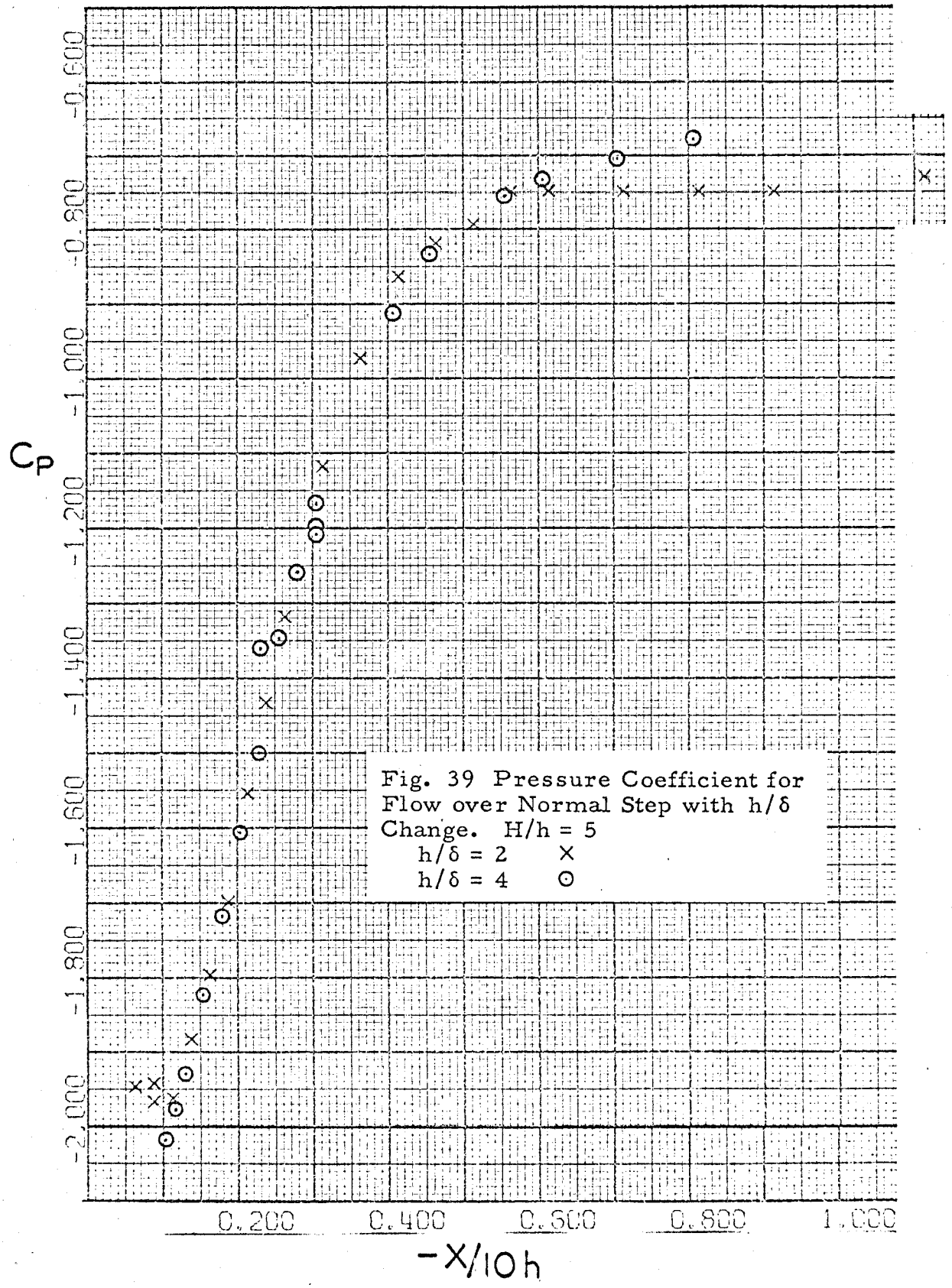

Fig. 39 Pressure Coefficient for Flow over Normal Step with h/δ Change. $H/h = 5$
$h/\delta = 2$ ×
$h/\delta = 4$ ⊙

indicate that the value of h/δ does not affect the far downstream (plateau) region. However, the data are too incomplete to fix a boundary layer thickness ratio influence on the near-field pressure level.

The effect of the external flow geometry on the downstream pressure field is illustrated by Figures 40 and 41. For Figure 40, $h/\delta = 1.0$, and $H/h \doteq 20$ for the circled data and $H/h = 10$ for the crossed data. As the interference of the step is increased (H/h decreased), for h/δ held constant, the pressure coefficient level in the plateau region far downstream becomes more negative with very little effect on the field near the step-top leading edge. This effect on the plateau region results from the increased velocity in this area due to the increased interference produced by step and cavity.

The effects of blockage and h/δ changes are summarized in Figure 41. The crossed data represent $H/h = 20$ and $h/\delta = 1$; the triangle data represent $H/h = 10$ and $h/\delta = 2$; and the circled data represent $H/h = 5$ and $h/\delta = 4$. Note that the plateau pressure coefficient becomes more negative as interference increases and that the pressure coefficients in the area near the step-top leading edge become much more negative as h/δ increases.

Figure 42 illustrates the influence on the plateau pressure coefficient downstream of the step by the external geometry for the actual data as compared with two possible mathematical models discussed in Section III. The inviscid case is for flow over a normal step with no cavitation, and the cavitating case is for the flow discussed in Section III, i.e., with dead water regions both upstream and downstream of the step. For the latter calculations, the single case for $C_{p_s} = 0.40$

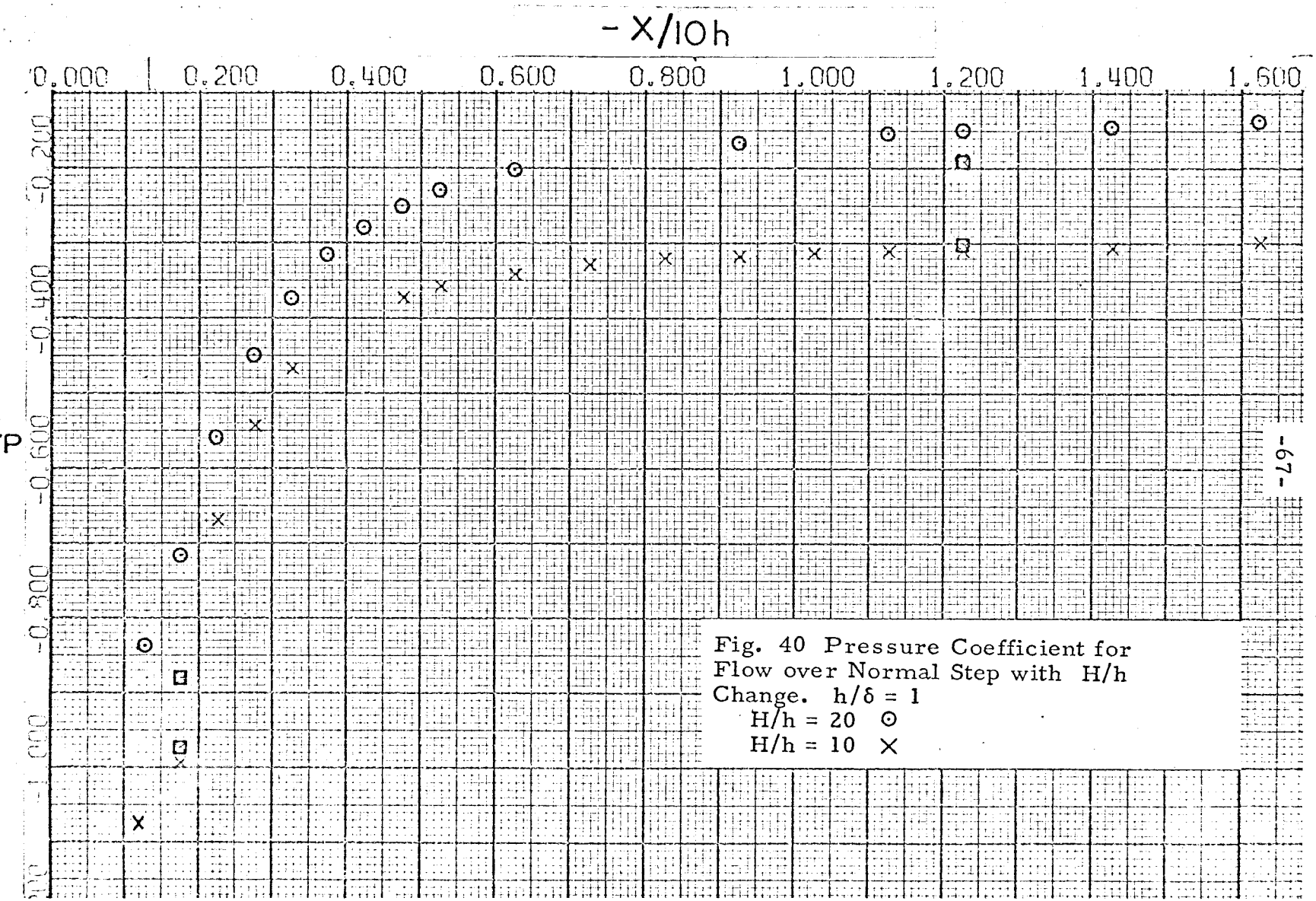

Fig. 40 Pressure Coefficient for Flow over Normal Step with H/h Change. $h/\delta = 1$
H/h = 20 ⊙
H/h = 10 ×

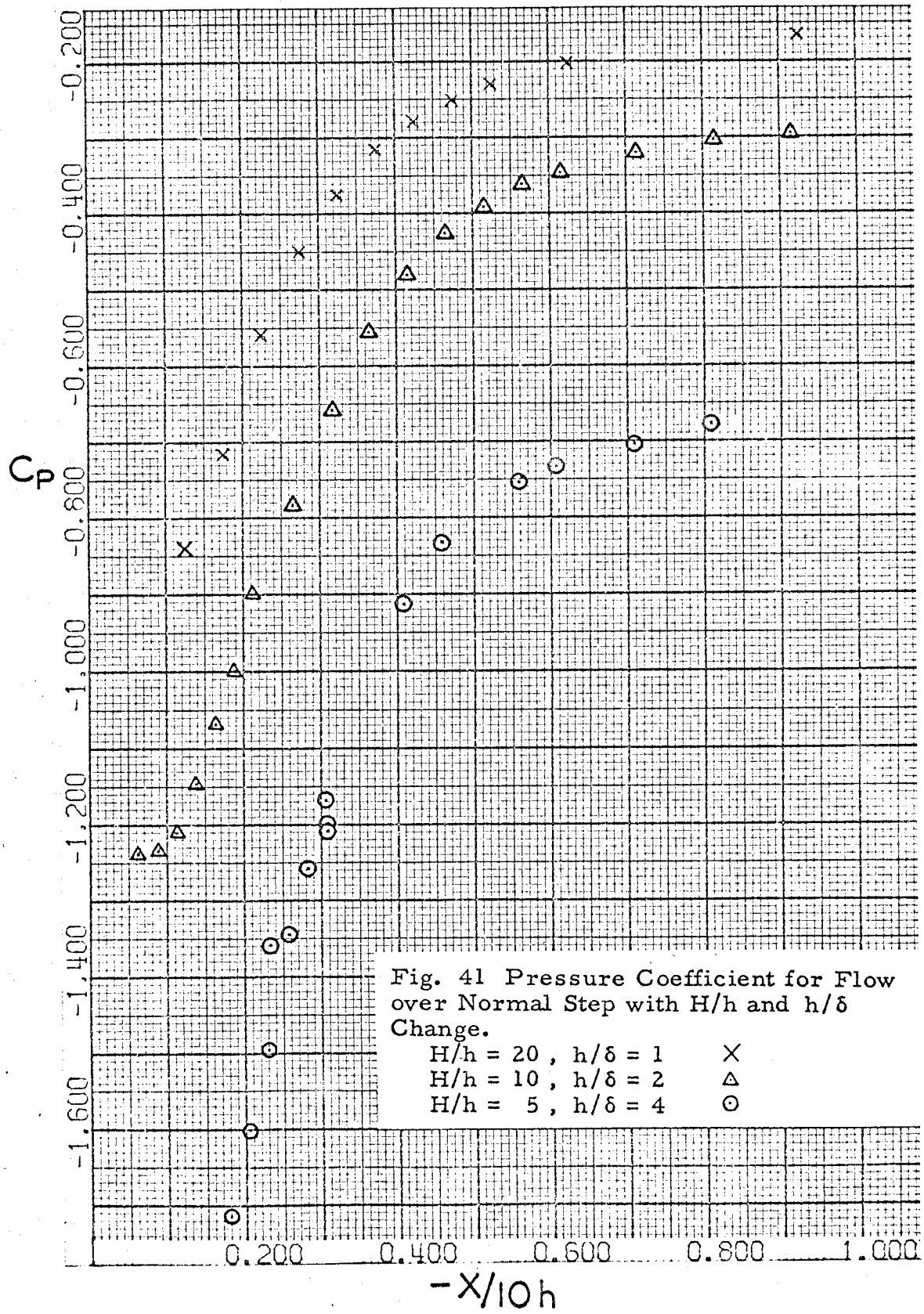

Fig. 41 Pressure Coefficient for Flow over Normal Step with H/h and h/δ Change.

H/h = 20 , h/δ = 1 ×
H/h = 10 , h/δ = 2 △
H/h = 5 , h/δ = 4 ⊙

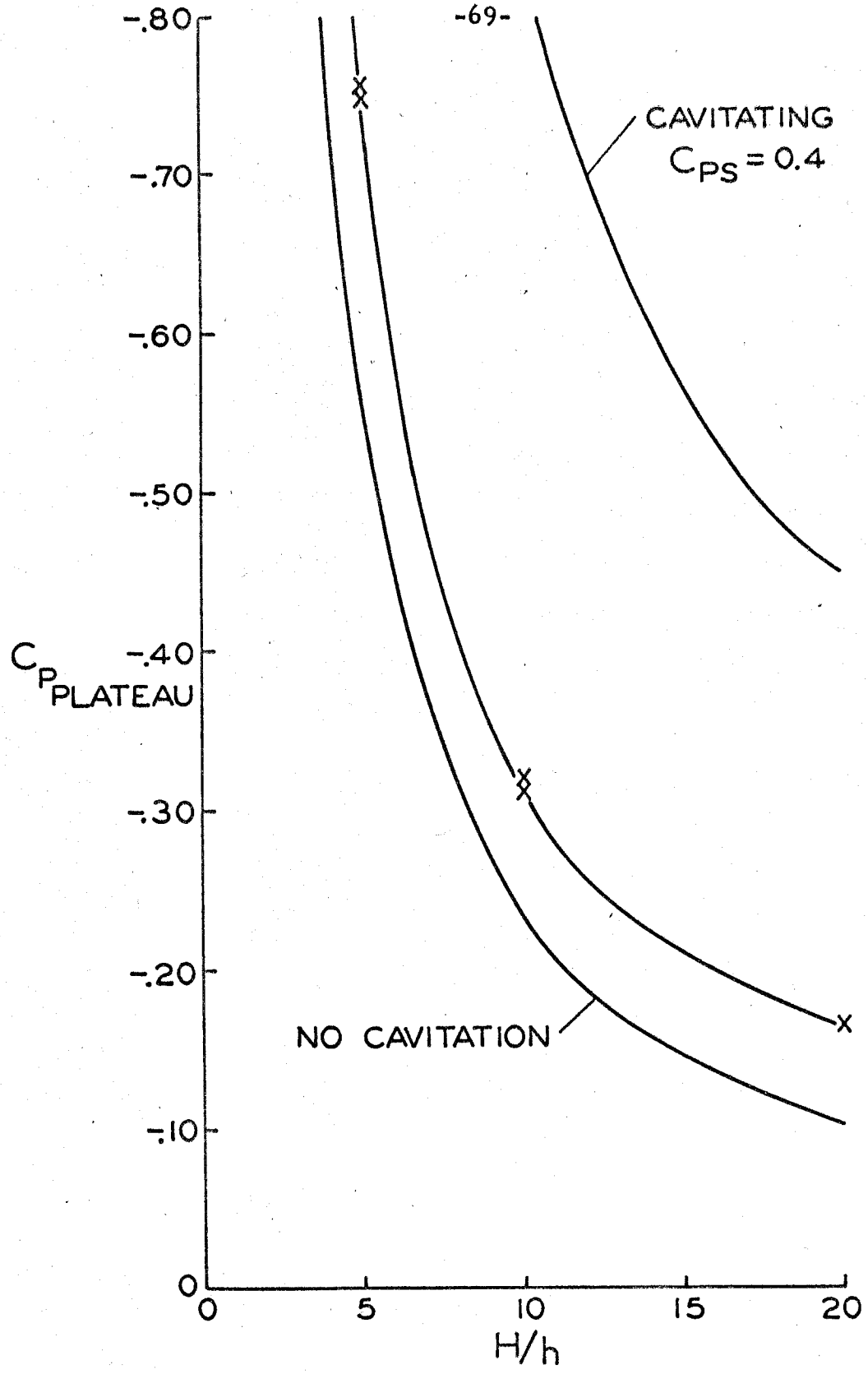

FIG. 42 PLATEAU PRESSURE COEFFICIENT ON STEP TOP

is shown. The crossed data indicate the plateau pressure coefficient for each of the blockages tested. It is evident that the actual flow in the downstream region must have a thinner mixing region than is predicted by the cavitating case. This was demonstrated earlier with Figure 36. Calculations based on continuity of flow and experimental values of the downstream plateau pressure show that the effective height of the step h' is roughly 1.22 to 1.3 h and that this value is independent of Reynolds number and blockage. Table V summarizes the data obtained in the present tests and shows that as h/δ increases the effective height decreases toward 1.22 h.

The location of the maximum negative slope of pressure coefficient curves was determined and shown on Figure 43. Within the accuracy of determining points, it appears that the location of the maximum slope scales as twice the step height and is independent of h/δ influence. A few visual observations indicated a reattachment point of about 3.5 to 4 step heights aft of the step leading edge.

Finally, note that the relaxation of the pressure to the plateau value is insensitive to blockage effects and that the scale of the entire downstream region appears to be the step height. Figure 44 demonstrates this very well for the 1-, 2-, and 4-inch step heights, where $\bar{C}_p = (C_p - C_{p_{min}})/(C_{p_{max}} - C_{p_{min}})$ is plotted as a function of $(-x/h)$. Note that all three curves agree reasonably well even though H/h changes from 5 to 20. The values for $C_{p_{min}}$ and $C_{p_{max}}$ are well defined for the 2- and 4-inch steps. Values for the 1-inch step were chosen as $C_{p_{min}} = -0.87$ and $C_{p_{max}} = -0.17$, and reasonable deviations from these values do not change the gross effect. As was ob-

h (inches)	L (inches)	H/h	U_o (ft/sec)	h'/h
1	68	20	10.39 14.87	1.46 1.30
1	68	10	10.30 12.58	1.17 1.26
1	38 1/4	10	10.28 15.18	1.27 1.20
2	68	10	10.37 14.87	1.25 1.21
2	68	5	10.26	1.21
4	68	5	10.26 13.96	1.23 1.22

TABLE V. RATIO OF EFFECTIVE STEP HEIGHT (h')
TO ACTUAL STEP HEIGHT (h)

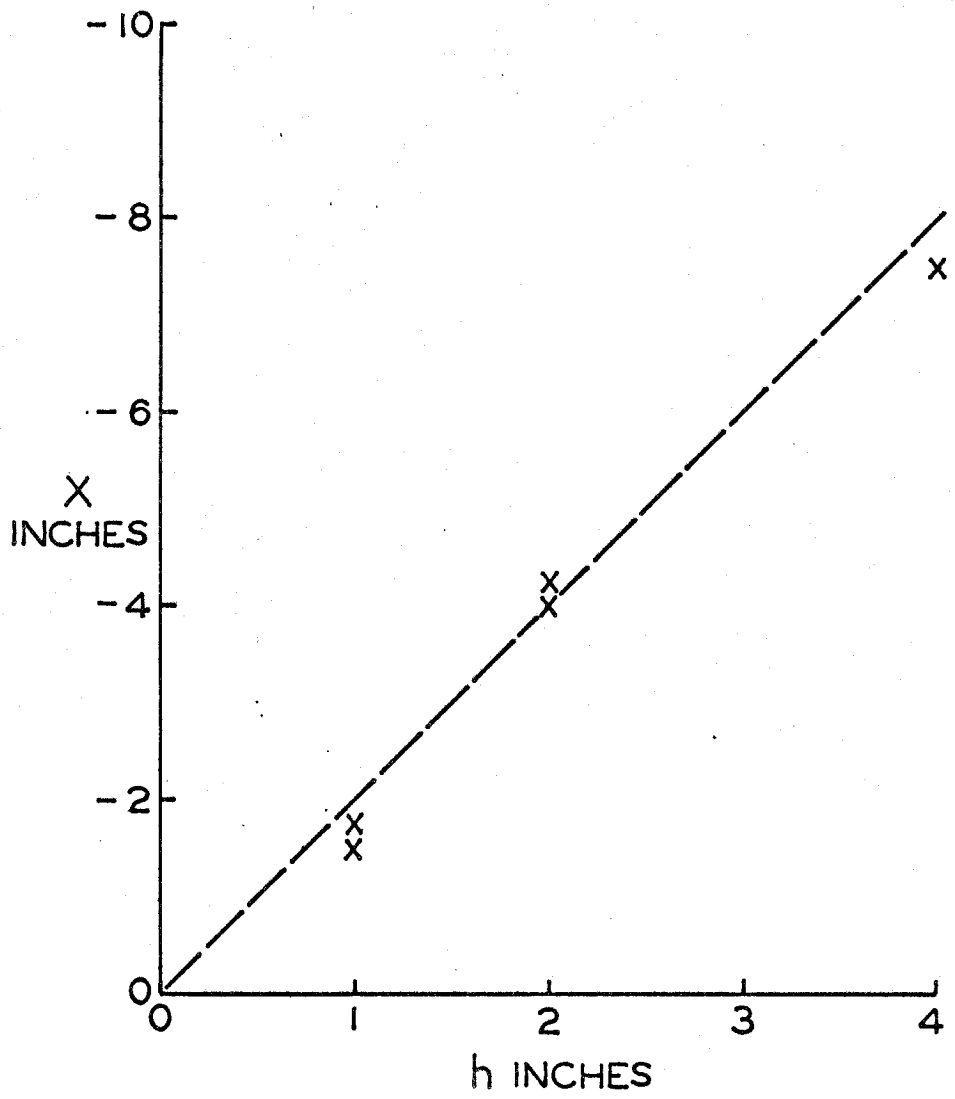

FIG. 43 LOCATION OF MAXIMUM CHANGE RATE OF PRESSURE COEFFICIENT FOR FLOW DOWNSTREAM OF NORMAL STEP

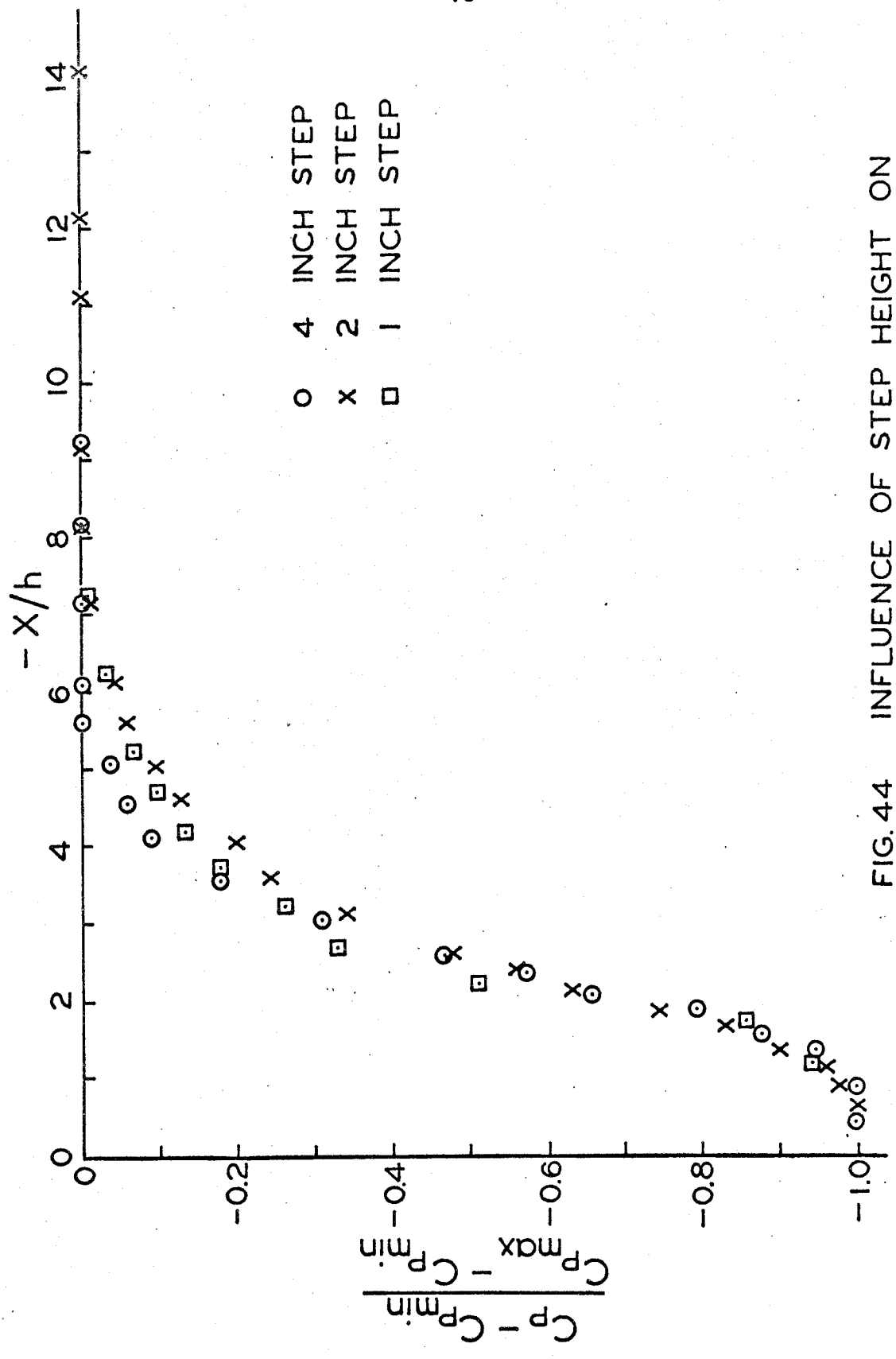

FIG. 44 INFLUENCE OF STEP HEIGHT ON DOWNSTREAM PRESSURE FIELD

served visually, the reattachment point was about 3.5 to 4.0 step heights downstream, and at this location the $\overline{C}_p$ rise is about 0.80 to 0.85. This is compatible with results that other authors have obtained with rearward-facing steps.

In summary, the scale of the downstream pressure field appears to be h, and changes in either h/δ or H/h ratios appear to have very little influence on the scale. Of course, the blockage (H/h) has a great effect on pressure coefficient values in general, and the initial boundary-layer thickness does appear to influence the minimum value of pressure coefficient at the step corner.

V. CONCLUSIONS

The results of the experimental data for incompressible flow over a forward-facing normal step in a channel indicate that the pressure field can be divided into two regions that are influenced by one or more characteristic parameters.

The pressure field in the base area upstream and downstream of the step is primarily determined by the effects of boundary layer interactions. These effects appear to depend in a systematic manner on the step height - to - boundary layer thickness ratio. There also is a lesser effect due to the external flow geometry, i.e., the ratio of channel height to step height.

The pressure field far upstream of the step is determined by the ratio of the channel height to step height. There, boundary layer effects are insignificant, and the region of boundary layer influence near the step decreases in size for increasing ratio of step height to boundary layer thickness. This result, convincingly documented here, is in marked contrast with that reported by Bradshaw[1] and Taulbee[2], who concluded that δ was the dominant scale in fixing the entire upstream pressure field.

The pressure field downstream of the step scales with the step height. The effective step height in this region is about 1.25 the actual step height, i.e., the displacement thickness far downstream of the step scales with the step height.

Although the measurements were crude and the location was unsteady, the separation and reattachment points also scale with the step height and are roughly independent of the ratio of channel height

to step height. For example, the separation point occurs about 1.3 to 1.6 step heights forward of the step; the reattachment point on the step face occurs about 0.5 step heights above the base; and the reattachment point on top of the step occurs about 3.5 to 4.0 step heights downstream of the step.

The pressure coefficients upstream, downstream, and on the step face are not influenced by Reynolds number for the threefold change studied in these tests. The pressure coefficients in the far downstream region are strongly influenced by the ratio of channel height to step height.

REFERENCES

1. Bradshaw, P. and Galea, P. V., "Step-induced Separation of a Turbulent Boundary Layer in Incompressible Flow," Journal of Fluid Mechanics, Vol. 27, Part I (1967), pp. 111-130.

2. Taulbee, D. E., "Separation of a Turbulent Shear Flow Ahead of a Normal Step," Ph. D. Thesis, University of Illinois (1964).

3. Chapman, D. R., Kuehn, D. M., and Larson, H. K., "Investigation of Separated Flows in Supersonic and Subsonic Streams with Emphasis on the Effect of Transition," NACA TN 3869 (March 1957).

4. Lighthill, M. J., "On Boundary Layers and Upstream Influence," Proc. Roy. Soc. A, Vol. 217 (1953), pp. 344-357.